

6YO Neck Dummy Design Project Final Report



Ben Randoing, Jia Yu Cheung, Leo Yeung, Will Taylor

BME432: Biomechanics and Vehicle Safety

Dr. Jason Luck

12/13/2021

Abstract

The purpose of the design project is to design a 6YO neck dummy that could biofidelically model the kinematics and mechanical behavior of the human 6 year old neck. The 6YO neck dummies are primarily used for researching and evaluating vehicle safety and products including booster seats and seat belts. Analysis of the current 6YO Hybrid III neck dummy by Sherwood *et al.* displayed multiple issues indicating that it is not biofidelic and representative of 6 year old injury response and kinematics. In addition, due to the lack of biomechanics data for pediatric research, the development of an accurate neck dummy could produce more models of the pediatric neck's biomechanical response. This report summarizes the design and iteration process undertaken to create the final design. The gross shape of the final design is a 109 mm tall cylinder sandwiched between two 5 mm thick steel plates. The inner neck consists of upper and lower butyl rubber sections with an inner ABR rubber disc. The ABR and butyl rubbers are connected by six titanium prongs superiorly and one wider titanium prong inferiorly. The upper steel plate consists of four holes to mate with the existing 6 year old neck, and the lower steel plate features holes to mate with the lower neck bracket. Figure 1 depicts the CAD design of the final neck including the lower neck bracket. The primary features of the neck were the unsupported superior segment of butyl rubber to allow for shear and biofidelic translation. Furthermore, the slanted ABR rubber disc facilitates the translational movement of the upper butyl rubber segment relative to the lower butyl rubber segment. When compared to the existing Hybrid III, these main features decrease the stiffness and support the biofidelity of the new neck by addressing concerns by Sherwood *et al.* An objective assessment of this final design produced the highest residual score (0.2797) and lowest correlation score (0.8217) yielding the lowest, and therefore best, overall score of 1.542.



Figure 1. Final Neck Design

Table of Contents

6YO Neck Dummy Design Project Final Report	1
Abstract	2
Customer and Clinical Need	4
Specifications and Constraints	8
Final Design	17
Final Testing Methods	22
Final Testing Results	24
Design Iterations	32
Applications Standards and Regulations	37
Ethical and Professional Responsibility in the Engineering Design Process	39
Convergence Study	42
Max Stresses	43
Future Modifications to Final Neck Design	45
Appendix	46

Customer and Clinical Need

The primary application of the 6YO neck dummy is the evaluation of vehicle safety and understanding the injury modes of the 6 year old neck in different loading conditions. The neck dummy is a crucial tool in assessing risk of both pediatric head and neck injury. Currently, pediatric cadavers are very limited in scientific research. In addition, there are large variances in anatomy and anthropometry with age and a lack of biomechanical data on pediatric necks. In order to continue addressing serious injuries and fatalities to child occupants in motor vehicle crashes, further development of child computational injury models and crash test dummies are needed.

Current available methods include the use of dummies, cadavers, computational modeling (finite element analysis), and animal surrogates (biomechanical scaling) in understanding neck injury and biomechanics.

The current 6YO hybrid III dummy is currently used in crash tests, however, it displays biomechanical characteristics that deviate from the human 6 year old neck. In Sherwood *et al.*, frontal sled tests displayed significant cervical spine flexion, allowing the head to contact the chest of the dummy. Thus, the sled test results show that the spinal response of the Hybrid III dummy under inertial loading is not biofidelic. In addition, the high overall stiffness of the neck dummy resulted in significantly higher neck forces and moments that are not representative of true injury potential. Furthermore, the 6YO Hybrid III neck dummy does not take into account posterior and anterior translation. A redesigned neck may be used by car manufacturers, roller coaster designers, or rocket scientists.

Cadavers are also a helpful tool in understanding neck biomechanics. Some of the advantages of using cadavers include correct anatomical structure, ability to establish injury thresholds, and soft-tissue injury. However, the limited availability of pediatric cadavers led to researchers turning to animal surrogates to approximate the response of child neck to load. One of the main limitations of this method is the differences in anatomical structure between humans and animals. As a result, researchers often use biomechanical scaling in order to approximate the appropriate neck injury and failure values using data derived from animal testing.

Another method used to research neck injury and biomechanics is computational modeling. Various studies, including Dibb *et. al*, build simulations of the neck and test the models under different tests including tension, compression, extension, and flexion. These simulations provide data relating to force, acceleration, displacement, and other metrics which can then be used to further study the neck.

When designing a novel dummy neck, public health, safety, and welfare are important to ensure the neck is compatible with societal expectations. Global, cultural, social, environment, and economic factors all influence the design of real products. These concerns for a dummy neck are detailed below.

Global

Typical vehicle collisions vary based on geographic location. Individuals in Dubai may experience rollover collisions near sand dunes. In contrast, individuals in Chile might experience falling down the side of a mountain. Provided the different potential crashes, loading conditions would vary immensely. The current neck featured a front NBDL sled collision which may be typical of collisions in civilized regions of the world; however, additional loadings conditions must be investigated should the product be implemented globally. Additional loading conditions may require the neck to be even less stiff and more biofidelic to ensure injuries are identified in simulations.

Similarly, the types of vehicles throughout the world vary significantly. There is an abundance of pickup trucks in the USA but many more compact cars throughout Europe. This difference extends to buggies and more open vehicles. Understanding the various loading conditions experienced in collisions involving each type of vehicle would influence the design of the neck. Designing a perfectly biofidelic neck has proven very difficult. That catering a neck to a specific population is essential to maximize the potential to protect individuals in different types of vehicle crashes.

Cultural

With many cultures throughout the world, there are sharp contrasts in the typical traditions, beliefs, and clothing people are accustomed to. This extends to beliefs about whether to wear neck protection or not. One way culture may affect the neck design is that specific protective gear may alter the way the neck and head respond to certain impacts. Understanding whether a culture emphasizes the need to wear a helmet or a neck brace is important in ensuring the neck models the conditions a real neck would be subject to in a specific culture. Furthermore, certain cultures are individualistic cultures whereas others may be collective. An individualistic culture is one in which people are less receptive to aid and are less willing to support others. Therefore, the culture may be less receptive to ideas presented by a separate country regarding novel devices and information. The country may not want to adjust safety standards as they believe their society is self-sufficient. Furthermore, certain cultures may believe in religions in which using crash test dummy data may be seen as combating the will of a higher power religious figure. These beliefs would be important to note to spread the information regarding a crash test dummy and safety standards for vehicles. The collective cultural differences also include whether females drive. If only males drive, the neck may be redesigned to tailor to a male neck.

Social

One of the biggest social factors to consider in the design of a biofidelic ATD neck is how well the neck performs under loading conditions that are representative of how the human neck will be loaded in the most common accidents experienced in society. It does not matter how well the ATD neck performs under varying loading conditions if the loading conditions are not representative of what will be experienced during a collision. In this way, it is important to understand what types of crashes are experienced most often and which of these causes the most severe injuries. The most up-to-date crash statistics should be used to determine the most common modes of impact loading. Current traffic laws and restrictions should also be considered from the perspective of what societal norms they are trying to moderate in order to prevent injury and death. Understanding this relationship will help guide design in a direction that protects the largest number of vehicle occupants.

Environmental

An important environmental consideration in the design of a new ATD neck is where crashes are occurring. The nature of a crash is fundamentally different between a low speed impact in a neighborhood compared to an impact taking place on a highway around a busy city. These collisions differ in their speed and potential loading condition, both of which have a large influence on the types of injuries that will be sustained. This is a similar consideration as the ones presented in the social factors guiding design. It implies that as engineers, awareness about the environment where collisions are occurring is of the utmost importance. Ideally, the design specifications used to prevent injury in high-energy impacts on a highway should ensure protection for occupants at lower-energy impacts like those that may be experienced in a fender bender. However, this is not necessarily true across all impacts, and loading conditions should be considered in order to account for this variability. An example of this would be the comparison between NBDL and CHOP tests used in this design. More weight was put on the higher impact NBDL collisions because this is where the most severe injuries would be expected, but to not consider the information presented by the CHOP tests would be engineering negligence. In future design, there should be more tests that share a similar relationship between NBDL and CHOP that account for scenarios other than frontal impact loading.

Economic

Economic factors associated with the design may include the cost of materials as associated with project budget and the allocation of available resources. The benefit of this design course specifically is the use of finite element analysis and computation modeling softwares including LS-DYNA and LS-PrePost, which allows the team to experiment with different designs and materials without the costs of building the prototype or design.

Some of the specific economic factors that should be considered include the potential impact to the local and US economy, the potential maintenance costs of the neck dummy, distribution costs, the ATD market analysis and the ease of manufacturing. Simple and easy manufacturing process is important for lower cost manufacturing. As a result, the design should have parts that are easily producible and assembled. This will allow for easier mass production, which can reduce cost associated with production. Another economic factor to be considered is the cost of goods sold. Costs associated with the type of material utilized in the neck dummy design should be considered in order to lower production costs. Thus, to further refine the current design, alternative cheaper materials may potentially replace the current Butyl rubber, ABR rubber, and steel used in the design.

In addition to the concerns detailed above, investigating prior patents of dummies and prior models is important to identify how successful aspects of other designs may contribute to a novel design. An example of an ATD neck design is detailed in a patent attributed to Humanetics Innovative Solutions Inc. as detailed in Figure 2. This neck design provides inspiration for the implementation of a revolute joint at the superior portion of the neck to support the initial absence of head rotation. Notably, the revolute joint does not comprise the entire cross-section of the neck and would be a way to implement a revolute joint with more stability. This could potentially fix the erratic movement artifacts in the detailed revolute joint iteration below.

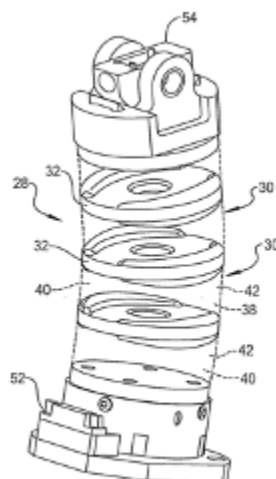


FIG 4

Figure 2. Patented ATD Neck by Zhenwen Jerry Wang

Another approach to increase the stability of the neck in the presence of a joint is to use a combination of joints. The ATD neck design initially assigned to BAE Systems Simula Inc. uses a torsion release swivel joint and pivot joint. These two components work together to help replicate the torsion, flexion, and extension behavior of the human neck. These joints also work together with an elastomeric beam to allow some forward and backward translation which was a point of emphasis guiding our own final design. Some of the main components such as the joints can be seen in the engineering drawing in figure 3.

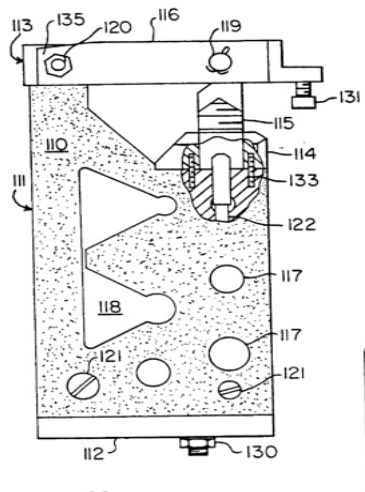


Figure 3. Patented ATD Neck by Marvin K. Richards

Specifications and Constraints

Students in the BME432/BME790 sections decided on the following performance specifications to use collectively as a group.

Tension Corridor

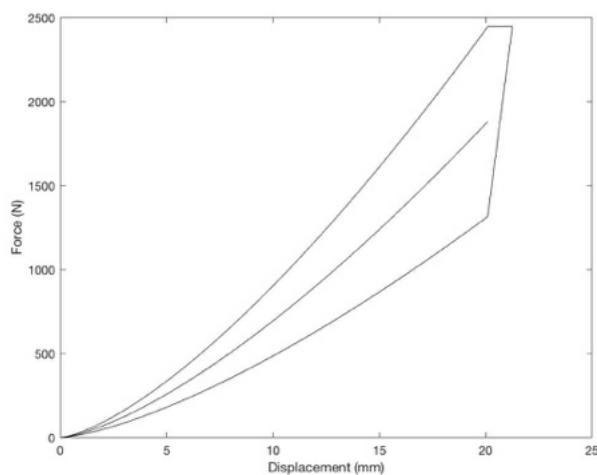


Figure 4. Class Tension Corridor

Compression Corridor

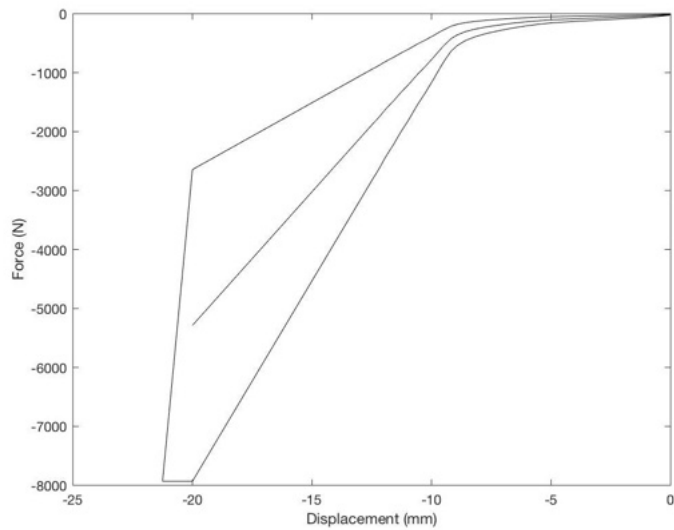


Figure 5. Class Compression Corridor

Flexion Corridor

Figure 6 depicts the Flexion corridor implemented throughout the class.

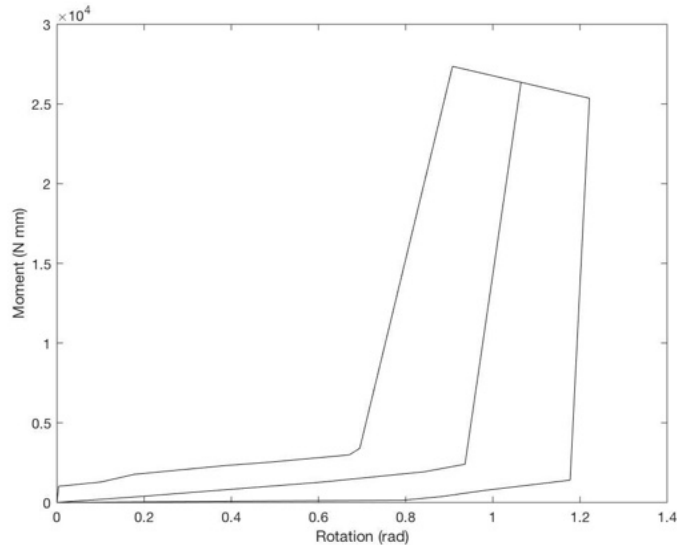


Figure 6. Class Flexion Corridor

Extension Corridor

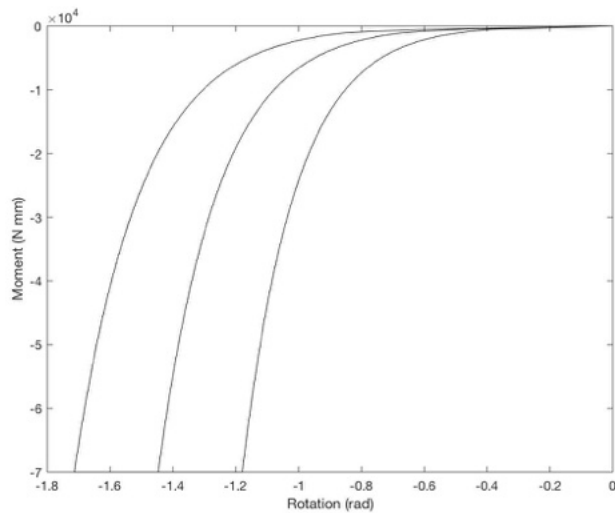


Figure 7. Class Extension Corridor

NBDL Corridor and Method

The NBDL corridors below in Figure 8 were derived by Thunnissen *et al.* after analyzing the behavior of a real human neck under a high impact sled test. The NBDL corridors focus on head and neck rotation in addition to head center-of-gravity displacement.

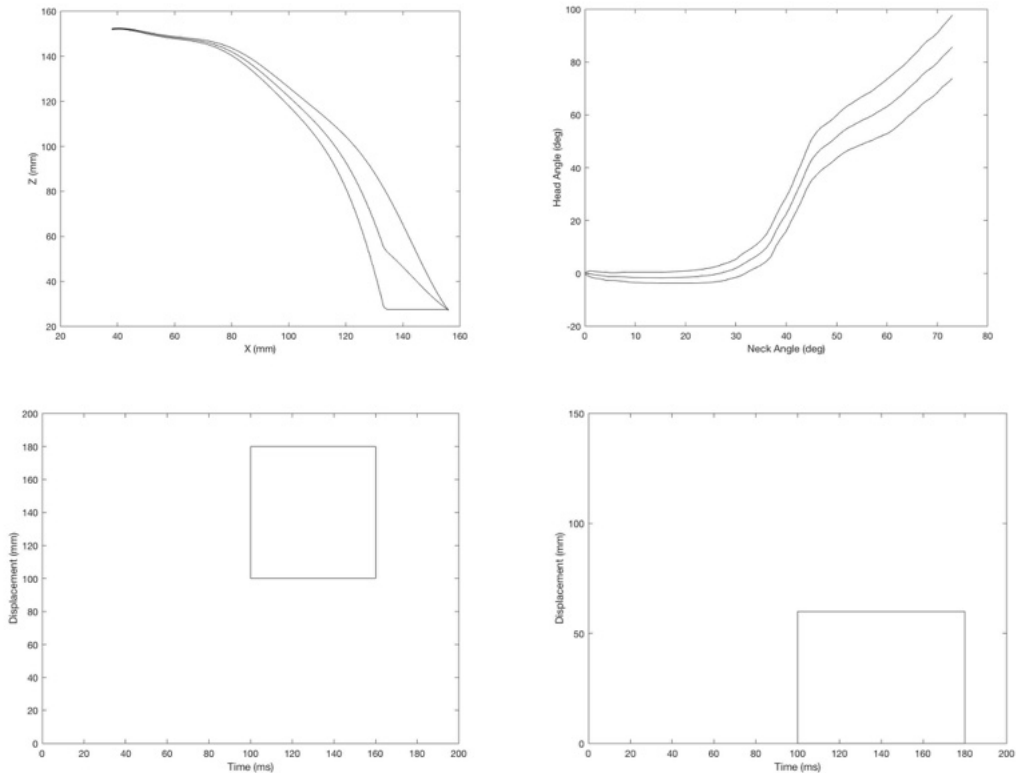


Figure 8. NBDL Corridors

CHOP Corridor and Method

The CHOP corridors in Figure 9 were developed by Arbogast *et al.* after subjecting subjects to a sled test at the severity of a bumper car impact. The displacement was identified at the external auditory meatus and the naion.

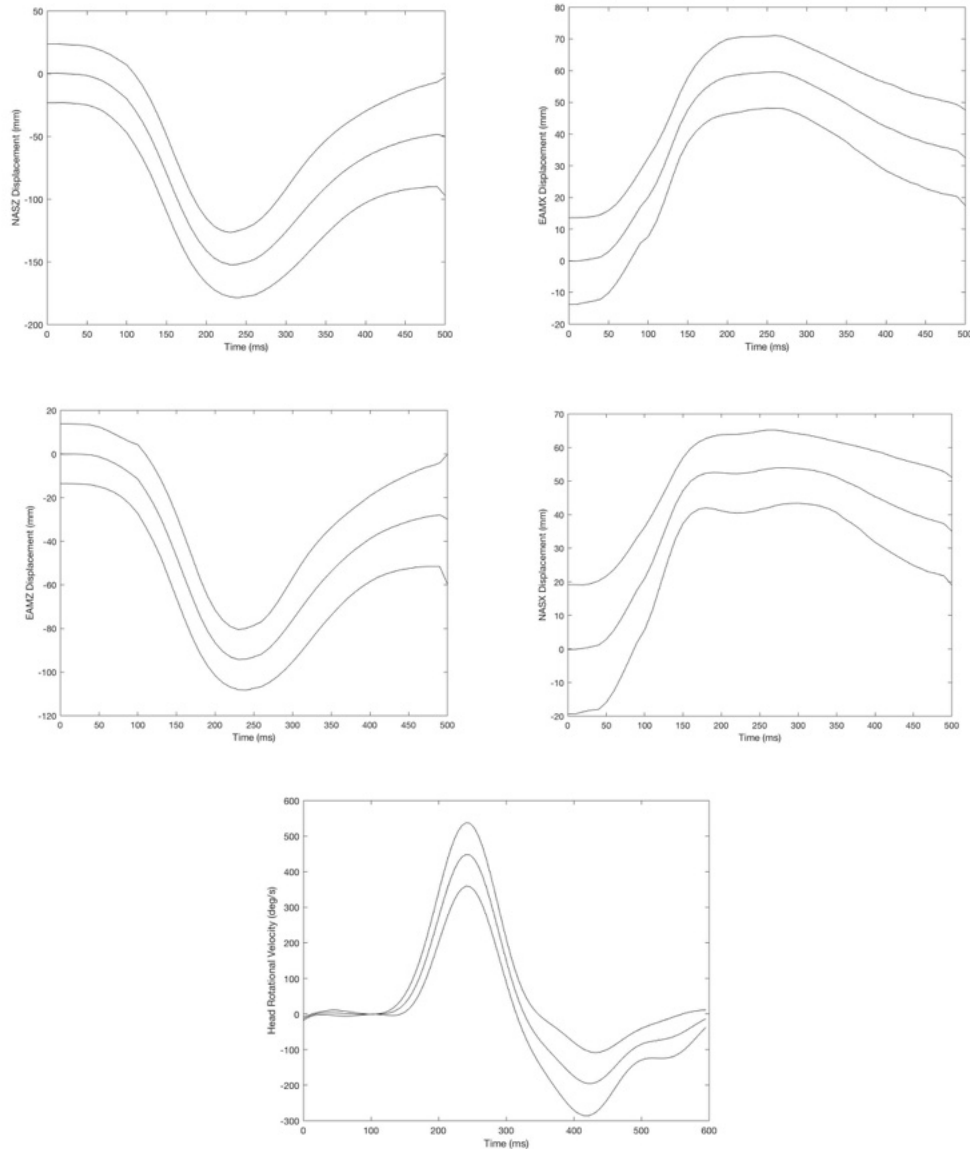


Figure 9. CHOP Corridors

Prior to choosing the corridors that every team would use in subsequent evaluation of the neck dummy performance, each team was responsible for creating tension, compression, flexion, and extension corridors and determining IARVs separately.

Team Capybaras Tension Corridor

Method:

Two main factors guided the design of the tension corridor for testing of the new neck design: using real data being tested in a similar fashion to the tests that will be applied in simulations and finding a way to include the effects of muscle. With this first factor in mind, an initial attempt at the corridor design was to treat the individual units of the spine as springs connected in series which would allow us to estimate the stiffness of the whole cervical spine. However, this method was abandoned because of the narrow nature of the corridor which would have been incredibly difficult to match in the simulations.

With this knowledge, the next attempt was to use data from Ouyang et al. in their destructive tensile testing of pediatric whole cervical spines. The specimens in these tests ranged in age from 2-12 years old, but our neck design is intended to be used with the 6YO Hybrid-III. Because of this, the data was normalized compared to the average of the two 6YO specimens' max force and max displacement. A mean load curve was then calculated by finding the average force at each displacement, and an upper and lower corridor were formed by adding or subtracting the corresponding standard deviation. At this point, the corridor needed to be scaled further to account for the inclusion of muscle. To do this, we used the tensile muscle tolerance range for adults supplied from Chancey et al. which was then scaled down using a scale factor for tensile force from Hilker et al. Once this scaled range was obtained, the normalized corridor supplied from the Ouyang data was scaled to make the maximum force equal to the average of scaled tensile muscle tolerance. The final corridor can be seen in Figure 10.

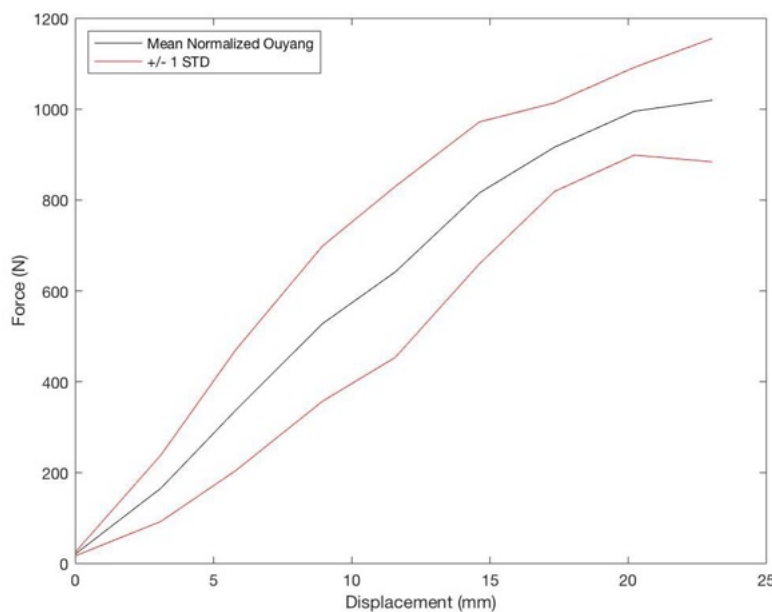


Figure 10. Tension Corridor Performance Specification

Team Capybaras Compression Corridor

Method:

Due to the lack of biomechanical data on pediatric neck in compression, metrics from different studies had to be combined to determine the compression corridor for the 6 year old neck. Based on the elastic limit and ultimate compressive strength values of different sections of the cervical spine from Przybyla et. al. Next, in order to get the slope of the corridor in between yielding and fracture points, overall stiffness values were derived from Nuckley et. al. Stiffness was estimated by modeling the sections of the cervical spine as springs in series with musculature in parallel with the cervical spine. Since these values were obtained from adult biomechanical data, the calculated force-displacement values had to be scaled to the 6 year old neck. A scaling factor for failure strength and yielding point was obtained from Eppinger and a scaling factor for stiffness was obtained from Hilker et. al. Finally, the mean \pm 95% confidence intervals of stiffness, elastic limit, and ultimate compressive strength

Compression Corridor:

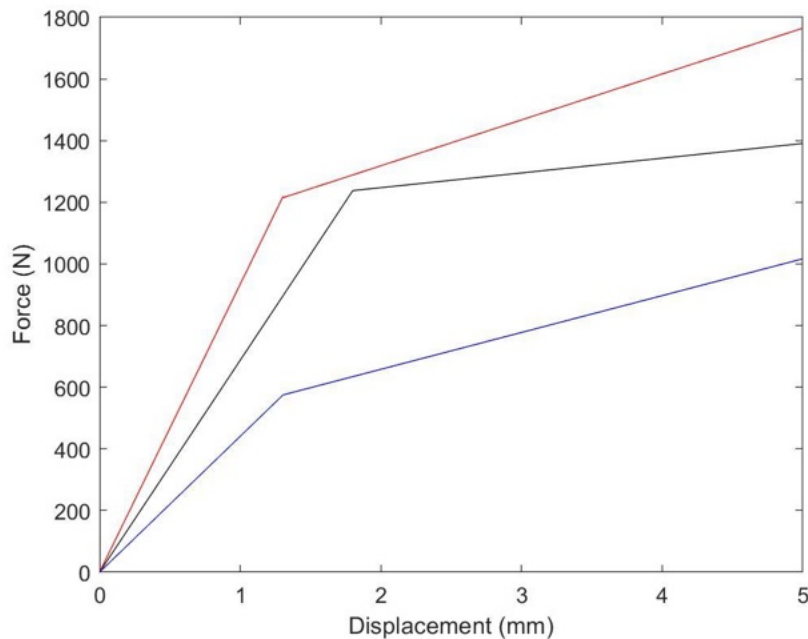


Figure 11. Compression Corridor Performance Specification

Team Capybaras Flexion Corridor

Method:

The flexion corridor was averaging the O-T2 moment-angle data from ten subjects in Ouyang *et al.* 2005. The data was from children aged 2 to 12 years; however, the bending stiffness of children within the appropriate age window in Nuckley *et al.* was consistent. Therefore, all patients were implemented. In addition to the average moment (Nm) and rotation ($^{\circ}$) relationship, the 95% confidence interval bounds were identified. After a spline regression fit the curves, the presence of the C7-T1 and T1-T2 joints were accounted for. Implementing a scale factor of 0.42 identified from a Caprine model in Hilker *et al.*, the adult moment-angle data for C7-T1 from Nightingale *et al.* and T1-T2 Wilke *et al.* were scaled and subtracted from the previous average and 95% confidence intervals. The IARV value identified below was appended to the corridor data to ensure it is included in the corridor.

Flexion Corridor:

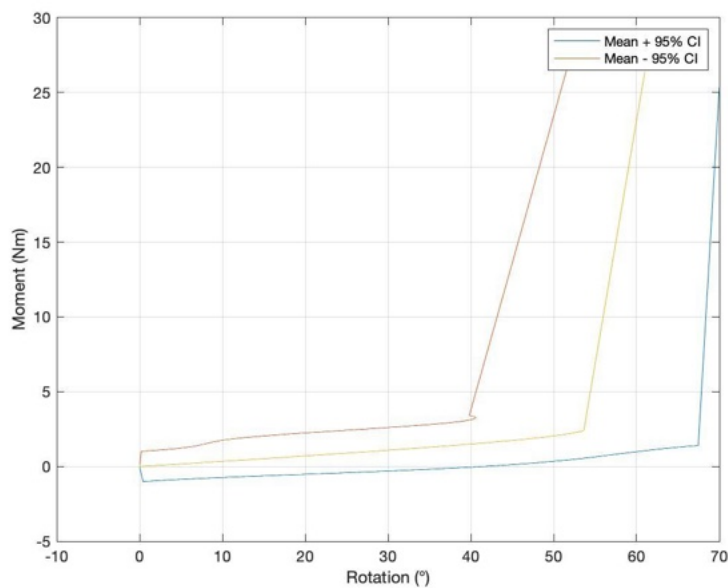


Figure 12. Flexion Corridor Performance Specification

Team Capybaras Extension Corridor

Method:

The extension corridor was developed with the same steps as the flexion corridor. The appropriate IARV was also appended at the end of the corridor data.

Extension Corridor:

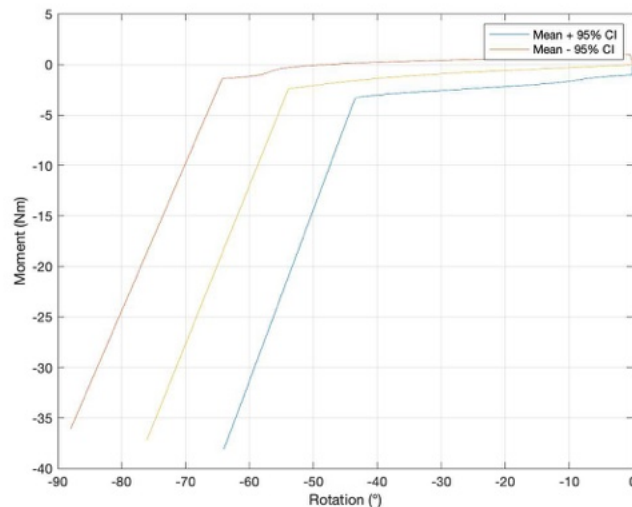


Figure 13. Extension Corridor Performance Specification

Team Capybaras Tension IARV

Method:

The tension IARV was obtained by modeling the neck as a set of springs in series. Luck *et al.* 2013 conducted tensile testing on pediatric osteoligamentous head-neck complexes across different developmental stages. The data for 6 year olds (72 months) were isolated and referenced. Data for ultimate failure was obtained for O-C2, C4-C5, and C6-C7. With the available data, the neck was modeled as a three-spring in series system, with each spring being each given segment of the neck. The displacement of each neck segment under ultimate failure was also noted in order to obtain segment stiffness using Hooke's Law. Given stiffness, displacement, and force, the segments were modeled in series and the overall ultimate force was determined to be 1336 N.

Team Capybaras Compression IARV

Method:

The compression IARV was obtained using literature values for the compressive tolerance of the whole cervical spine and the lower cervical spine. Due to a dearth of data on compressive strength of the upper cervical spine, the neck was modeled as a two spring in series system, with the upper and lower cervical spine comprising the system. Nightingale *et al.* 1997 reported the whole cervical spine under pure compressive loading to fail at 2243N on average. Using data of lower cervical spine failure loads provided in Carter *et al.* 2002, the upper and lower cervical spine failure loads are 2730N and 1239N, respectively.

Table 1. Tension and Compression IARVs

	Upper Cervical Spine	Lower Cervical Spine
Peak Tension Load (N)	1761	894
Peak Compression Load (N)	2730.5±1133.6	1239.2±268.9

Team Capybaras Flexion IARV

Method:

The flexion IARV was identified by first calculating a scale factor between the known failure loads for the C6-C7 vertebrae in adults and children from Nightingale *et al.* 2007 and Chancey *et al.* 2003. The scale factor of 0.49 was applied to known adult failure moments for O-C2, C4-C5, and C6-C7. These three data points were regressed to approximate the failure loads of the C2-C3, C3-C4, and C5-C6 connections. With known pediatric neck range of motion values from Arbogast *et al.* the stiffnesses of the UCS and LCS were identified by dividing the failure moment by the failure angular displacement. These stiffnesses were combined assuming the elastic modulus and moment of inertia of the neck remained the same. Additionally, the neck length was assumed to double; therefore, the final stiffness was the average of that of the UCS and LCS. This final stiffness was multiplied by the failure angular displacement to obtain and failure moment quantity.

Team Capybaras Extension IARV

Method:

The method for calculating the extension IARV was identical to that for the flexion IARV with the exception of accounting for muscle. Mertz and Irwin *et al.* demonstrated a 5 Nm lower IARV for the neck under extension; therefore, the calculated extension IARV was subtracted by 5 to provide the final IARV.

Table 2. Flexion and Extension IARVs

	Upper Cervical Spine	Lower Cervical Spine
Peak Flexion Moment (Nm)	32.65	26.36
Peak Extension Moment (Nm)	53.35	37.11

Final Design

Final Neck Design and Mechanical Features

The final neck design is illustrated in Figure 14. Additionally, a complete set of engineering drawings and a parts list may be reviewed in Appendix B.

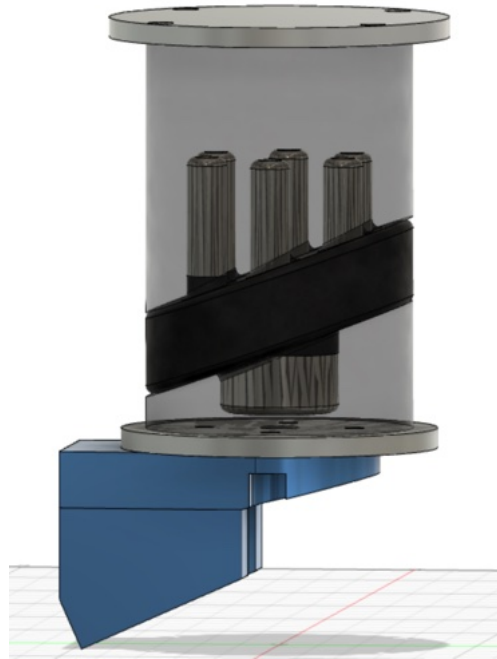


Figure 14. Final Neck Design

The final neck design attempts to reduce the overall neck stiffness and maintain appropriate relative stiffnesses between the upper and lower cervical spine. A description of the motivation and implementation of each key feature may be noted in Figure 15 and Table 3 below.

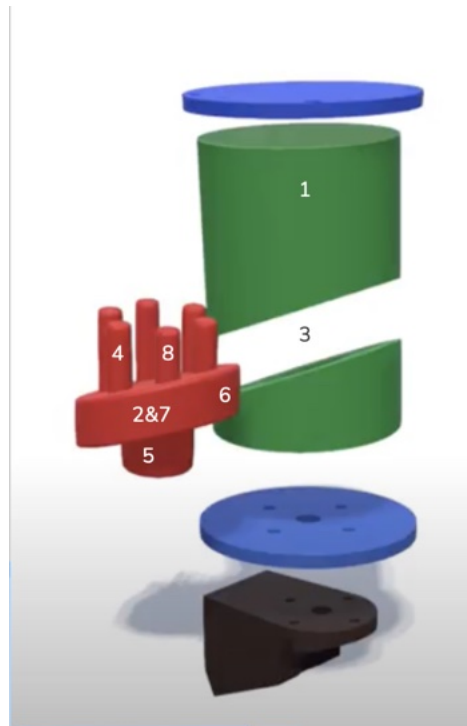


Figure 15. Color Coded Final Neck Design

Table 3. Motivation for Key Design Features

Motivation	Feature
Sherwood <i>et al.</i> 2003 - Lack of A-P Translation Contributes to High Neck Stiffness	1. Prongs Do Not Extend to Top Plate - Shear 2. Forward Slant in Middle ABR Rubber - Forward Compression 3. ABR Rubber Mid Section is Below Center Point
Ouyang <i>et al.</i> 2005 - Desired Increased A-P Bending Stiffness in UCS	4. Upper Prongs are Decentralized ($I = I_{cm} + md^2$)
Luck <i>et al.</i> 2013 - Desired Increased Tension and Compression Stiffness in LCS	5. Net Cross-Sectional Area of Prongs is greater for Lower Prong (706 vs. 471 mm ²)
Desired Increased Stiffness in Flexion vs. Extension	6. Superior End of Slanted ABR Rubber is Anterior
Desired Strain Stiffening Response in Compression	7. Use of ABR Rubber in Mid Region and Butyl Rubber in Top and Bottom
LS-DYNA Requires Rigid Bodies Between Deformable Materials	8. Titanium Prongs

A key feature of the final neck design was not having the titanium prongs extend to the top steel plate. This allowed additional flexibility in the top butyl rubber segment. Sherwood *et al.* mentioned the need for A-P translation, and the uninhibited butyl rubber may allow for increased shear and potential translation. By moving the titanium prongs away from the center, the cylindrical moment of inertia was greater than having a single centralized prong. In flexion and extension, stiffness is directly proportional to moment of inertia. Therefore, the upper cervical spine would feature an increased moment of inertia in accordance with Ouyang *et al.* Range of Motion quantities in Arbogast *et al.* indicated the neck was slightly stiffer in flexion rather than extension. This was clear in the corridors as well. Therefore, the ABR rubber insert was slanted forward toward the anterior region of the neck. This increased the stiffness of the neck under flexion.

Total CPU Runtime and Deformable Elements

The final neck mesh implemented a triangular auto mesh element size of 3 mm. This resulted in 28112 total deformable elements in the combined neck model. Furthermore, the CPU runtimes for all six test conditions are presented in Table 4.

Table 4. CPU Runtimes for Final Simulations

Test	CPU Runtime (s)
Tension	3610
Compression	3643
NBDL	8982
CHOP	13095
Flexion	7868
Extension	7978

Total Neck Mass

The mass of each component of the final neck design is presented in Table 5. The total mass of the assembly, excluding the lower neck bracket, was 691.8 g. This quantity was calculated using Fusion 360.

Table 5. Final Component and Assembly Masses

Component	Mass (g)
Total Assembly	<u>691.8</u>
Inner Foam and Prongs	247.3
Top and Bottom Butyl Rubber	30.4
Bottom Plate	191.4
Top Plate	222.7
Lower Neck Bracket	253.7

Final Neck Design Strengths and Weaknesses

The strengths and weaknesses of the final neck design are presented in Table 6. The most significant successes were the overlap of the compression corridor at high displacements and the general high overlap of the extension corridor. However, our neck was weakest in the NBDL head lag and overall tensile profile. The neck featured strain softening in tension and demonstrated too much head rotation too early with respect to time.

Table 6. Strengths and Weaknesses of the Final Neck Design

Strengths	Weaknesses
Meets Compression Corridor at Large Displacements	Absence of Strain Stiffening in A-P Bending
Meets Tension Corridor at Medium Displacements	Significant Head Rotation too Early in NBDL Head Lag
Maximum Head CG Displacements during NBDL are within Bounds	Not Enough EAM X and Z or NAS X Displacement from CHOP
Ease of Assembly	Rigid Metal Prongs are Not Entirely Realistic
Meets Most of Extension Corridor	Metal to Rubber Connection is a Weak Connection
	Titanium Cost & Low Mass
	Too Stiff in Early Tensile and Compressive Loads

Final Testing Methods

Tension

A tensile test constituted connecting the superior and inferior faces of the neck design to rigid bodies. The inferior body was fixed, and the superior body was specified by a double haversine function for acceleration. The two rigid bodies were constrained to the outermost rigid bodies in the neck iteration. The most superior body would begin movement to apply a tensile load to the neck. This was important to resemble the biofidelity of an actual collision. The torso of an individual would be fixed and the load would be applied as the head moves away from the body.

Compression

A compression test followed the same procedure as the tensile test; however, the loading curve was inverted. Therefore, the movement of the most superior rigid body resulted in the compression of the neck iteration.

Flexion

Flexion testing was designed to impart a moment on the neck rather than an axial force. By applying a time acceleration profile to the lower neck bracket in the anterior direction, the neck was flexed. The top and bottom plate of the neck were defined as rigid bodies. When following the lower neck bracket movement in post-simulation animations, the head would appear to move. The objective of applying the load to the lower neck bracket was to resemble the head moving relative to the torso.

Extension

Extension testing followed the same procedure as the flexion test. The difference is that the load was applied in the posterior direction to simulate head-neck response in the case of neck extension. The moment was now applied so that the neck was extended.

NBDL

The NBDL frontal collision test was established by applying an acceleration profile with respect to time to the lower neck bracket. The neck was fastened to the existing Hybrid III head and torso in the LS-DYNA simulations as well. The acceleration profile was determined from a sled acceleration profile applied to cadavers in Thunnissen *et al.* In this test, the superior end of the neck was rigidly connected to the head and the inferior segment of the neck was rigidly connected to the lower neck bracket. The lower neck bracket was rigidly connected to the torso. The NBDL and CHOP loading conditions were implemented in the negative x direction facing the posterior end of the neck to capture the head acceleration profile identified in experimentation.

CHOP

The CHOP frontal collision test applies an acceleration time profile to the lower neck bracket. The acceleration time profile was obtained from low speed frontal sled tests to male volunteers with a lap and shoulder belt system attached within the work of Arbogast *et al.* 2009. The rigid connections of the CHOP tests were analogous to those in the NBDL simulations. Furthermore, the acceleration profile was implemented onto the lower neck bracket to achieve the appropriate loading condition onto the neck.

Final Testing Results

Simulation/Testing Data

The performance of the final neck design with respect to all performance specifications may be observed below. RS stands for residual score and CS stands for correlation score.

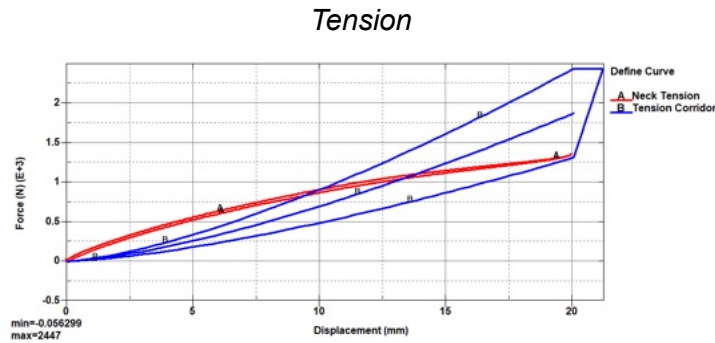


Figure 16. Final Neck Performance under Tension (RS: 0.2418; CS: 0.0843)

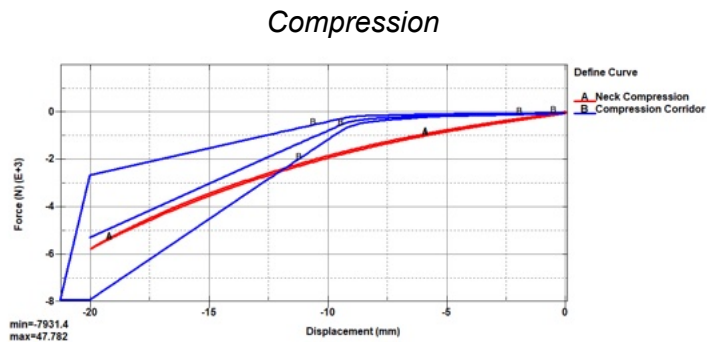


Figure 17. Final Neck Performance under Compression (RS: 0.2547; CS: 0.4160)

NBDL

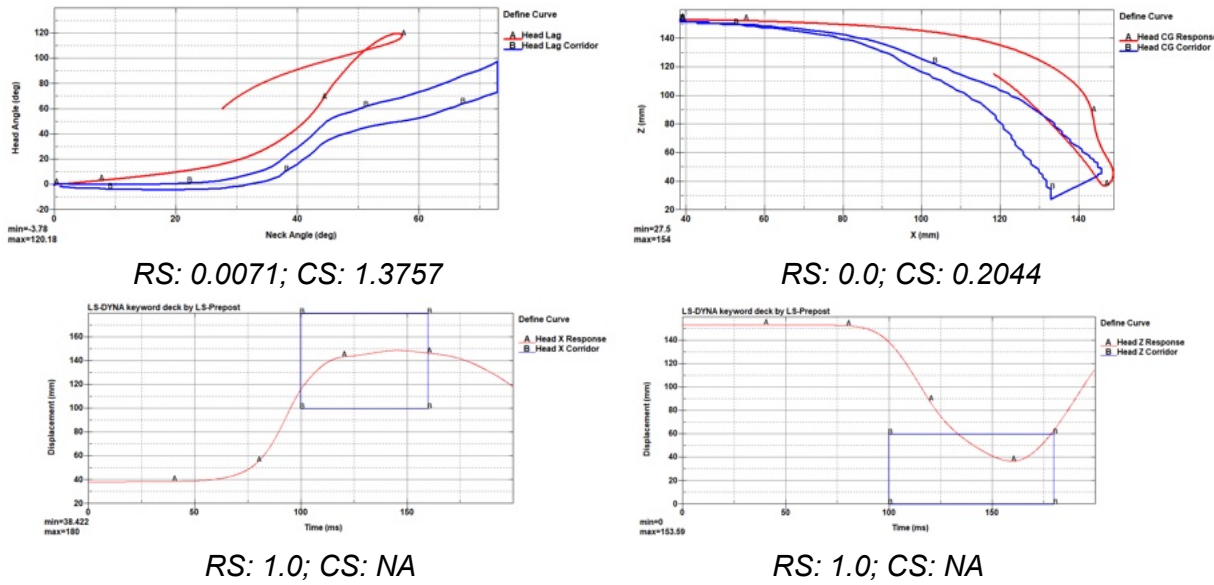


Figure 18. Final Neck Performance NBDL

CHOP

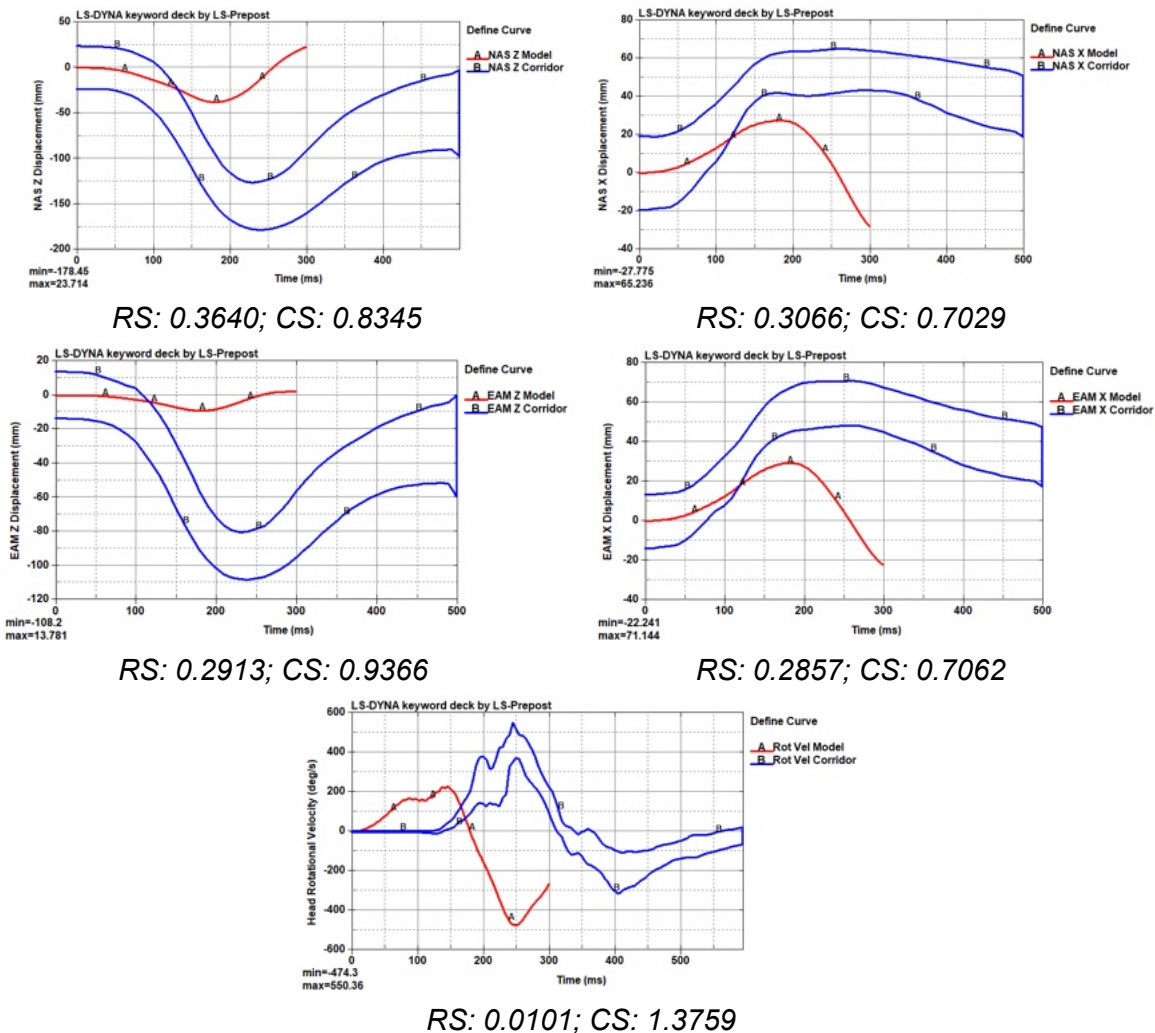


Figure 19. Final Neck Performance CHOP

Flexion

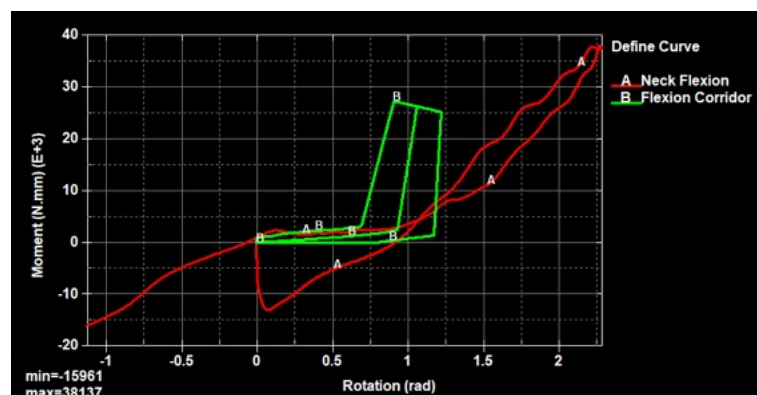


Figure 20. Final Neck Performance under Flexion (RS: 0.0212; CS: 1.4904)

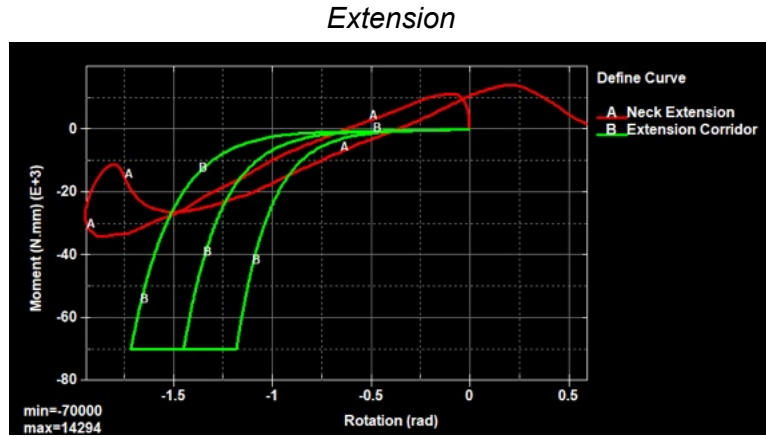


Figure 21. Final Neck Performance under Extension (RS: 0.3538; CS: 0.9978)

Objective Assessment

In creating our own objective assessment, current literature describing objective assessment of biomechanical data was reviewed. The method that was determined to be most applicable to the data obtained from simulations were those detailed in the use of the CORA method. This was comprised of what will be referred to as a residual method and correlation method. The residual method was used to compare the distance from the simulation data to the relevant corridors, and the correlation method was used to compare the shape of the simulation data to the shape of the mean corridor curve.

Producing Corridor Fits

Before either of these methods could be applied, the corridors had to be modified in a way that would make them suitable for comparison to incoming simulation data. To accomplish this, fits were developed for every curve in each corridor. The x-values of the simulation data could then be used to regenerate the corridors to allow for a point by point comparison. The general approach to generating fits for the corridors was to split the data from the correlation curve files into lower and upper curves (and a mean curve if it was supplied) and then use the curve fitting app in MATLAB to produce coefficients and equations that could be used to recreate the corridors. A summary of the fits and R^2 values for each curve can be seen in Appendix E.

There were several notable exceptions to this general method, but this did not interfere with the production of curve fits. For compression, the curves consisted of a set of points from -12.44 mm to 0 mm and included a maximum force at -20 mm. Because of this, 20 points were included in the form of a straight line between the forces occurring at -20 mm and -12.44 mm. This then gave enough points for the curve fitting app to produce a reliable set of fit coefficients.

For flexion, there were not enough points to use the curve fitting app, and the curves did not end at the same amount of rotation. The app also would not have produced a fit that would accurately describe the piecewise nature of the curves. Because of this, each curve was split into individual sections and extended to 1.222 rad if necessary. The upper curve was represented by two lines (one from 0 to 6.948 rad and another from 6.948 to 1.222 rad). The lower curve was represented by three lines (one from 0 to 0.7938 rad, one from 0.7938 to 1.177

rad, and the last from 1.177 to 1.222 rad). The mean curve was represented by two lines (one from 0 to 0.9362 rad and another from 0.9362 to 1.222 rad).

For extension, the exponential nature of data raised concerns for application of the residual method. Because of this, fits were generated with the general fitting procedure for each curve, but a cutoff was applied to crop the curves at a maximum rotation of -1.2 rad.

For the CHOP corridors, mean curves were not supplied, so they were generated by taking the average of the upper and lower corridors at each point. The CHOP head rotation curve also contained noise that made it difficult to use the curve fitting app. Looking at the article where the curves were obtained, it appeared as though this noise was likely due to outliers in the 6-8 year old group, and the three other sets of data for older age groups displayed the same general shape without noise. Because of this, the noisy section of data from 150 to 250 ms was removed, and the new set of data was then fitted using the curve fitting app. This preserved the peaks and peak locations of the curves, and it produced a corridor similar to those shown in the older age groups.

The original set of points for the NBDL CG displacement corridor was stepwise in nature meaning that there were several y-values assigned to one x-value. This made it so the curve fitting app could not be used to generate fits. Because of this, the first y-value at each x-point was preserved while any redundant points were removed. The upper corridor also extended further in x-displacement than the lower corridor (146 mm compared to 133 mm), so the lower corridor was assumed to be equal to its last supplied z-displacement (27.5 mm) in this range. Mean curves were generated for both NBDL CG displacement and head lag by taking the average of the upper and lower corridor curves. All curves were then extended to a displacement of 156 mm to create a fully enclosed corridor of accepted displacement.

The corridors supplied for NBDL CGx and CGz timing were boxes indicating where max displacement was supposed to occur in the data, so curve fitting was not necessary in these cases.

Residual Method

For each test, all of the data followed the same general procedure: isolate loading portion of curve, interpolate data using the interp1 command in MATLAB to obtain 500 linearly spaced points, use the simulation x-values to recreate corridors using fit coefficients, take the difference from simulation data to mean curve, and determine residual score at each point and average across all points to obtain a final residual score for the test.

Residual scores range from 0 to 1 such that a 0 is outside the corridor, and a 1 exactly matches the mean curve. For points within the corridor that did not exactly match the mean curve, the residual score was obtained by dividing the distance between the mean curve and simulation data by the distance from the mean curve to the outer corridor curve.

Again, the unique nature of each set of data led to some notable exceptions to the general residual method procedure. In the cases of tension and compression, the loading curve was determined by removing data that occurred after the maximum displacement. A small subset of points also had to be removed from the beginning and end of each set of data because MATLAB was considering them as non-unique points (likely due to rounding because the differences were so small). This meant that the first and last 50 points were removed from the tension data, and the first 15 and last 40 points were removed from the compression data.

This number of points was chosen on a case by case basis between tests to ensure that as much simulation data was preserved as possible.

In the case of NBDL head lag, the loading curve was isolated by removing points occurring after the maximum neck angle. In some cases, the data was cropped again if this maximum neck angle was greater than 80 to avoid going past the limits of the corridor. A similar process was used for NBDL CG displacement, but data was cropped to not go past 156 mm x-displacement. The first 20 points were also removed to avoid repeating x-values. In some cases, the data still had non-unique points at higher displacements because all movement was being experienced in the z-direction instead of the x-direction. In these cases, the data was cropped beyond the point where the non-unique points began occurring. The NBDL CG timing data was much different from the other tests because the corridor was much different. Only the maximum point in each curve was assessed, and the assessment of this point was based on whether or not the point occurred within the supplied corridor box. This meant that a 1 was given if the max of the curve occurred within the box, and a 0 was given if the max occurred outside of the box.

For flexion and extension, the loading curve was isolated by removing data that occurred after the maximum rotation. The data was then further cropped for each test to avoid going past the regions where the corridors could be compared to each point. In the case of extension, this meant data was only compared up to a maximum rotation of -1.222 rad. In the case of flexion, this meant data was only compared up to a maximum rotation of 1.2 rad.

Correlation Method

For each test, all of the data followed the same general procedure: autocorrelate the mean corridor curve with itself, cross-correlate the simulation curve with the mean curve, sum all points in each correlation, and find the percent error between the two sums using the autocorrelation sum as the reference value.

Percent error did not range from 0 to 1, but it was constrained to only positive values. In this case, values closer to 0 indicate a lower amount of error and greater similarity between the simulation and mean curves. Because of the data modifications that already took place during the residual method, all data was already prepared to be correlated, and there were no notable exceptions to the general procedure outlined above.

Determination of Overall Score

To compare between design iterations, it was desirable to have one overall value instead of comparing the residual and correlation scores separately. To accomplish this, a weighted average was used to combine the results from each individual test. Weighting factors were determined based on a literature review of modes of impact and their relevance to injury prevention. The final weighting factors can be seen in Table 7. The weighting factors were determined through literature review of injury mechanisms for frontal collisions. Forward flexion of the neck was found to be a common mode of neck injury in frontal collisions (Kullgreen 2000). Therefore, flexion was given a weight of 0.20. NBDL was given the highest rating due to the nature of a sled test resembling real world collisions. In addition, the NBDL sled test operated with higher acceleration sled testing, which would allow for more conservative measures of quantifying neck injury. The final residual score was determined by multiplying the scale factor

by the average residual value for each set of tests (tension, compression, flexion, extension, NBDL, and CHOP) and then taking the sum of all these values. The same procedure was used for the final correlation score, but NBDL CG timing tests were not included in the NBDL average. These values were then combined by summing the correlation score and the difference between the residual value and 1. This produced a final score greater than 0, such that the lowest value was considered to be the best match to the corridors.

Table 7. Weighting Factors for Combination of Testing Results

Test	Weight
Tension	0.15
Compression	0.125
Flexion	0.20
Extension	0.125
NBDL	0.25
CHOP	0.15

Strengths and Weaknesses

This objective assessment criteria has several strengths and weaknesses. The first strength is that the same number of points is being compared in each test. In this case, 500 points were used, but this number can be easily modified to increase or decrease precision. Another strength is that the points are linearly spaced. The raw data from the simulations had varying densities of points in upper and lower regions of the curve, so interpolating the data was crucial to ensure that all portions of the curve were assessed equally. Another benefit to the overall setup of the objective assessment code is that it is easy to modify individual sections of the code. The variability among sets of data meant that it was important to be able to make small changes within each test if necessary. The code is organized in a logical manner and makes it easy to go in and run the assessment on individual tests. The objective assessment also does not take long to run and very little modification of the crv files is necessary before running the full assessment.

There were also some limitations to the objective assessment. The first limitation that was the most relevant was the requirement of unique points. This was needed for both the interp1 command and the MATLAB curve fitting app. In most cases, this meant removing the first or last section of points that had such small differences between one another, that MATLAB considered them to be the same point. Removing these sections did not affect the overall assessment of the curve. The main situation where this became an issue was in the NBDL head lag and CG displacement graphs. Some of these curves had non unique points in the middle of the data, which made it difficult to remove them. Because of this, the data was cropped to exclude these portions of the data, but this also meant that the full curve was not being assessed. Another point of concern was how to assess the NBDL CG timing graphs. In these

tests, only one point was being assessed, and the only possible scores were a 1 or 0. This gave these graphs a heavier influence on the residual score. The code should be modified to decrease this influence by making the difference between the values smaller (0.5 for the maximum not occurring in the window instead of 0) or assessing them separately from the residual method.

Another limitation to the objective assessment was the use of the correlation score. This was originally intended to compare the shape of the simulation curve to the mean curve. However, this method actually described the difference in overall size. The percent error method used to compare the correlations gave the same values as percent error difference for average y-value of the simulation curve and mean curve. In future implementation of this objective assessment, another comparison should be added to compare differences in x-values for a more complete comparison of shape. One possible way to do this would be to compare where the max correlation point occurred. The correlation method also needs to be normalized. The percent error approach supplied values greater than 0, but it would be better if the values were constrained to be between 0 and 1. This would make it so the residual and correlation scores would be producing values within the same range which would allow them to contribute to the overall score equally.

The final limitation to this objective assessment was that there was not a specific criteria for rejection. The goal was to produce iterations that gave an overall score closest to 0. Because of this, it was easy to compare between iterations to see which ones matched the corridors better. However, there was not a specific cutoff for a highest allowable overall score. Instead, most of the rejected iterations were based on more subjective measures such as whether or not a specific change to the design was producing the desired behavior or if the model was stable under all of the tests.

Design Iterations

V5 with Revolute Joint

After recognizing the erroneous head rotation of the final neck design, a revolute joint was implemented with two butyl rubber wedges to prolong the time until the head began to rotate. Figure 22 depicts the CAD model of the design iteration, and a complete set of engineering drawings for the revolute joint iteration may be observed in Appendix D.

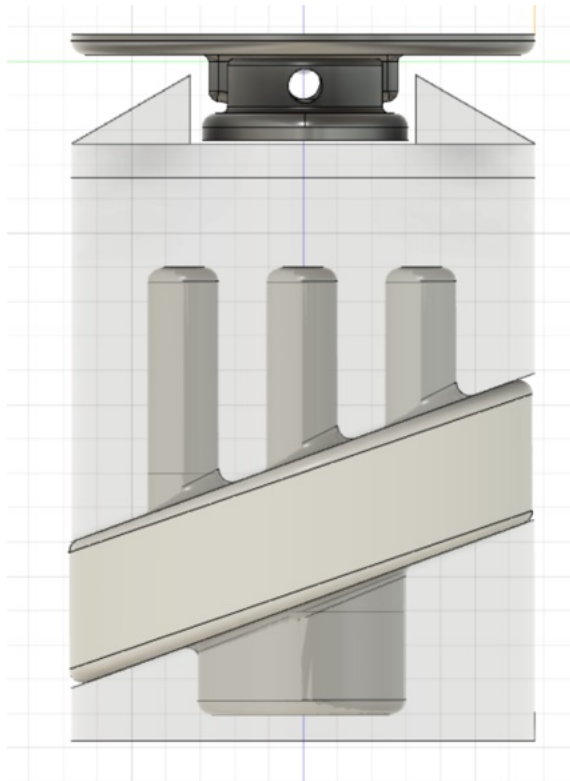
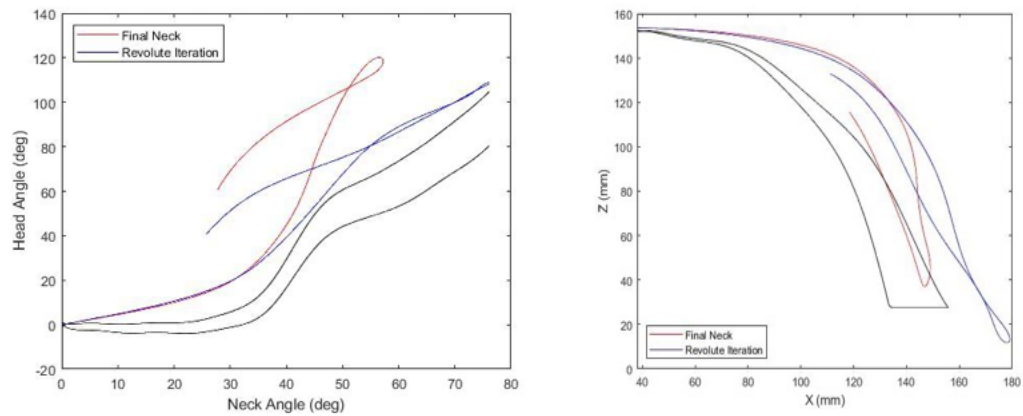


Figure 22. Revolute Joint Iteration

The revolute joint iteration did not prove to reduce the early head rotation as observed in Figure 23. Furthermore, the neck demonstrated greater head center-of-gravity displacements, which may result in the neck erroneously hitting a car seat in front of the test dummy. Additionally, the joint led to undesirable behavior of the joint under compression as observed in Figure 24.



Final RS: 0.0071; Revolute RS: 0.0049

Final CS: 1.3757; Revolute CS: 0.5039

Final RS: 0.0; Revolute RS: 0.0

Final CS: 0.2044; Revolute CS: 0.2416

Figure 23. NBDL Comparison between Final and Revolute Joint Necks

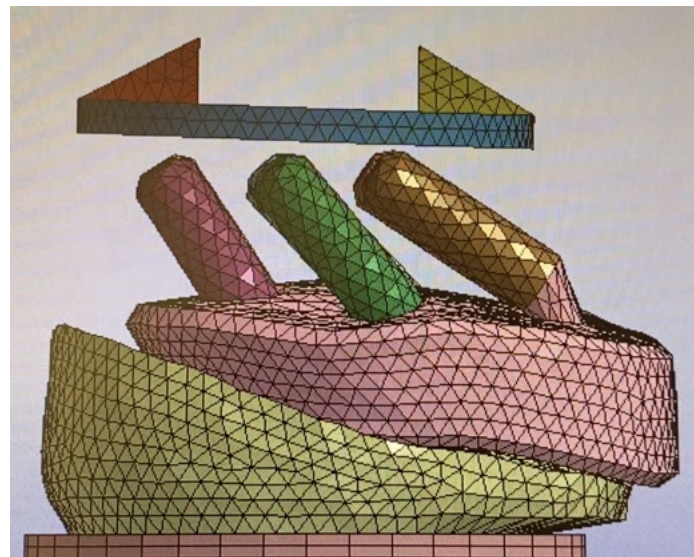


Figure 24. Undesirable Behavior of Revolute Joint Iteration under Compression

V5 with Translation Joint Prongs

To address the large stiffness of the final neck design at early displacements under tension and compression, the 6 titanium prong above the ABR rubber disc were converted to translation prongs. Figure 25 depicts the translational joint design iteration.

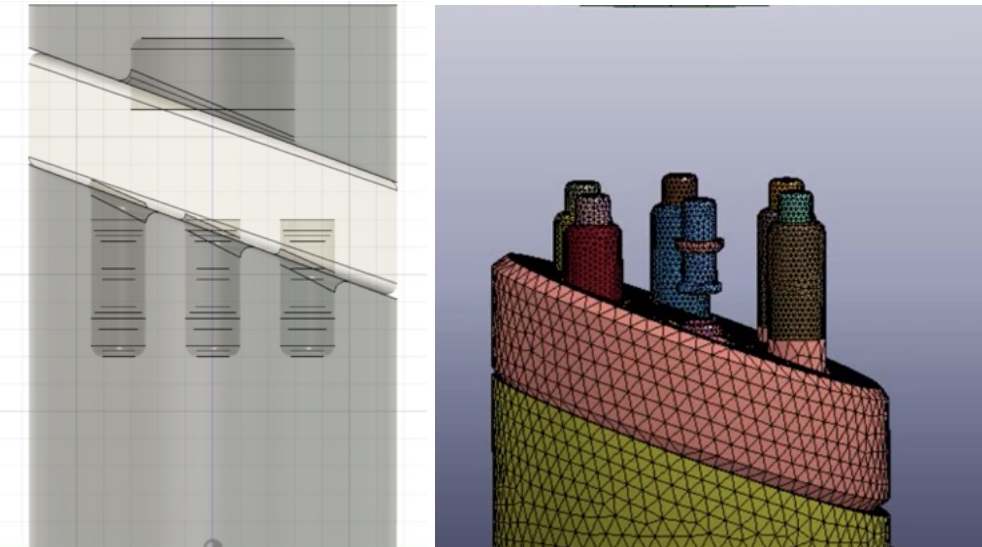
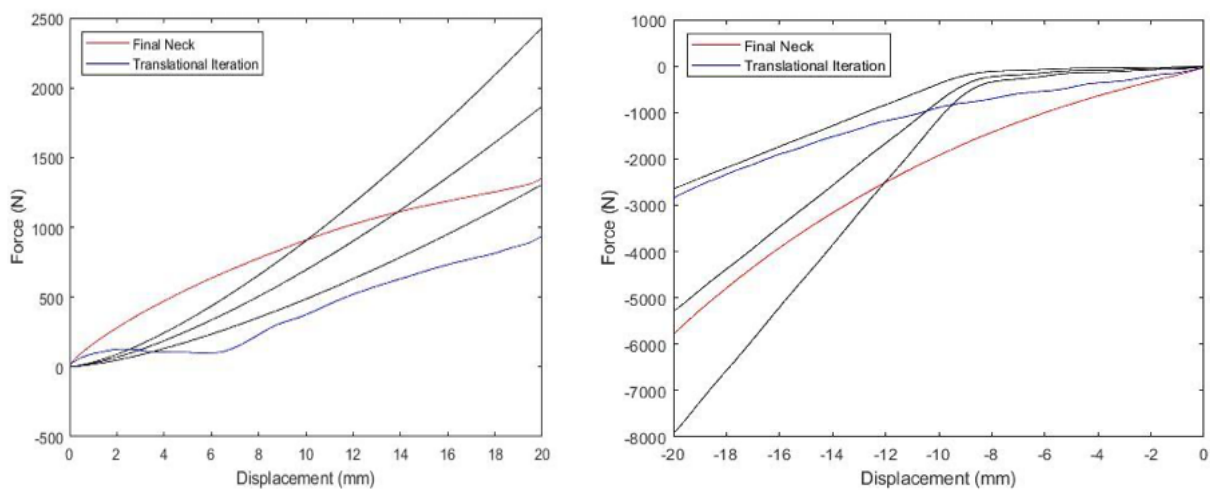


Figure 25. Translation Joint Neck Iteration

The translational joint demonstrated promise in both tension and compression as observed in Figure 26. Under tension, less translational distance is needed and the joint should be moved to the top of the design to avoid any initial stiffness from pulling on the butyl rubber. Under compression, the neck would need to stiffen to a greater extent following the full movement of the translational joint. Provided more time, this iteration may be honed to improve upon the current final neck; however, the presented low stiffness and lack of overlap with the corridors in Figure 26 resulted in the translational joint neck being discarded.



Final RS: 0.2418; Translate RS: 0.0225
Final CS: 0.0843; Translate CS: 0.4649
Final RS: 0.2547; Translate RS: 0.1362
Final CS: 0.4160; Translate CS: 0.3045

Figure 26. Tension and Compression Comparison between Final and Translational Necks

V2: Nuclear Power Plant Design

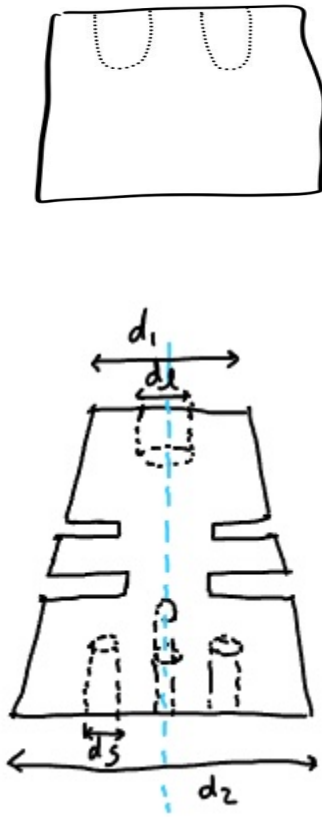


Figure 27. Nuclear Power Plant Sketches

Initially, the nuclear power plant design was utilized to examine the impact of adding holes of different lengths and positioning in a solid. This design was guided by the following equations:

$$\delta = \frac{PL}{AE} \quad (1)$$

$$I_{hole} = I_{CM} + Ad^2 \quad (2)$$

The rationale behind the addition or repositioning of holes was based on multiple factors. The first concept that was considered was cross-sectional area at different z-distances throughout the neck. To account for the higher stiffness of the lower cervical spine compared to the upper cervical spine, the cross sectional area of the top of the neck dummy was made smaller. Further, to simulate the strain stiffening behavior of the neck in compression, straight and angled slits were added.

After the simulations, the data showed that the model did not demonstrate strain stiffening in tension or compression. Thus, the wide slits were sectioned out and replaced with rigid steel material as shown in Figure X. To further improve on the biphasic, strain-stiffening behavior of the model in compression, a burn-through section made out of 6YO Rubber was added at the top of the model. The rationale behind adding this section was that in compression, during the low-loading phase, the burn-through material, due to its compliance, can be burned

through to simulate low stiffness in low load. Once the burn through material is sufficiently compressed, the model will then display increased stiffness as the rest of the neck model (butyl rubber body and rigid steel slits) are compressed.

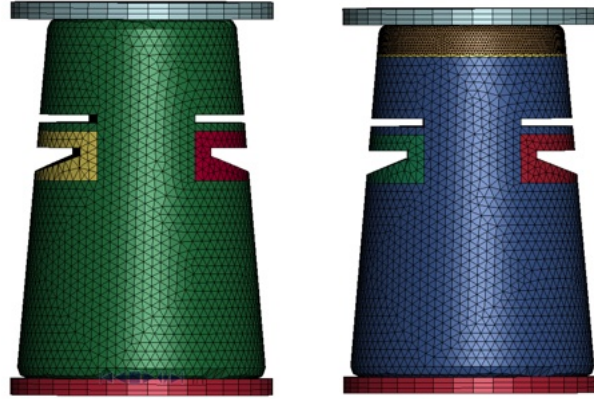


Figure 28. Nuclear Power Plant LS-PrePost Model

Following this iteration, the team decided not to proceed with design. The first reason was due to issues relating to the burn through material during simulation. LS Pre-Post would terminate the simulation once the burn-through material was compressed to a certain point, preventing the team from looking at the compressive behavior of the neck model in high loads. The second reason was the model's behavior in NBDL. Compared to other designs being investigated, this model significantly deviated from the performance specifications outlined in NBDL.

The final residual, correlation, and overall scores for the V5 iterations can be seen in Table 8. Other versions are not included because the designs were either rejected due to undesirable performance, or a full set of tests was not completed for these iterations.

Table 8. Objective Assessment Summary

File Name	Final Residual Score	Final Correlation Score	Overall Score
V5 (Titanium Prongs)	0.2797	0.8217	1.542
V5 (Steel Prongs)	0.2102	0.8836	1.6734
V5 (Shorter Prongs)	0.1196	0.9202	1.8006
V5 (1st Revolute Joint Iteration)	0.1928	3.1184	3.9256
V5 (Final Revolute Joint Iteration)	0.237	1.1184	1.8814
V5 (Translational Joint Prongs)	0.1664	0.9061	1.7397

Applications Standards and Regulations

Evaluation Process - Federalization

This process involves a standardized set of inspections and tests that provide quantified measures and corresponding documentation of the dummy's assembly/ disassembly, certification test procedures, durability, repeatability, reproducibility, and biofidelity. A candidate ATD or crash test dummy must undergo an evaluation and documentation process before it is incorporated into Part 572 of the Code of Federal Regulations. This process involves thorough dummy and drawing inspection, establishment of dummy's certification criteria, evaluation of dummy's biofidelity, and a detailed manual for the dummy assembly process. During the Federalization process, because of the high costs associated with crash testing and sled testing, some engineers choose to perform those tests after the less expensive inspection and lab tests. For the neck dummy, durability of the dummy can be tested in the lab, on a sled test, or in crash tests. During the inspection process, the dummies are acquired and completely disassembled and inspected. This includes checking the weights, CGs, and dimensions of the component segments. Figure 29 outlines the different federalization objectives.

		TASKS			
		Dummy Inspection	Lab Testing	Sled Testing	Crash Testing
FUNCTIONS	Drawing Package				
	Certification				
	Durability				
	R & R				
	Biofidelity				
	PADI				

Figure 29. Federalization objectives versus scheduled tasks matrix

Biofidelity Ranking

The Biofidelity Ranking System (BioRank) has been implemented in different studies since 2002 to assess the biofidelity of anthropomorphic test devices and model responses against a human response. BioRank has advantages over other objective metrics such as CORA or ISO/TS 18571 because CORA and ISO/TS 18571 assess similarity between multiple responses, thus, biofidelity is only assessed via comparative biofidelity. BioRank is a two part system that first assesses the biofidelity of individual ATD response measurements, and then combines those measurements via an averaging scheme to assess overall ATD biofidelity. A lower score is more desirable. BioRank takes into account acceleration in the x, y, and z direction, test conditions, and appropriate weighting to calculate the overall score.

Regulatory Agencies and Pathways

1. National Highway Traffic Safety Administration (NHTSA)

The NHTSA is responsible for assigning motor vehicle safety standards to reduce deaths and injuries resulting from traffic accidents. The National Traffic and Motor Vehicle Safety Act of 1966 requires each Federal Motor Vehicle Safety Standard (FMVSS) to be practicable, meet the need for motor vehicle safety, and be stated in objective terms. The NHTSA enforces compliance to FMVSSs by conducting crash tests with ATDs in the front onboard seats.

2. Department of Transport (DOT)

The Department of Transport (DOT) is making a concerted effort to develop an improved dummy neck due to the lack of biofidelity of the Hybrid-III neck both in flexion, extension, and axially. Since the inception of the Traffic Safety Act of 1966, the DOT has been trying to address the total fatality problem. The Department of Transport is often responsible for creating the technical report documentations that outline the seating procedure evaluation and revision for dummies.

Ethical and Professional Responsibility in the Engineering Design Process

There are many ethical and professional responsibilities engineers face when designing novel products. The redesign of a six-year-old neck presented above would need to be evaluated with respect to ethical standards prior to reaching the market. These ethical standards are detailed below.

Global

A core principle of medical and research ethics is justice. A core component of justice is to ensure all humans are represented as equally as possible in the development of new technologies. The resources for research should be distributed equally. The formulation of performance specifications based on component loading conditions during collisions in developed regions of the world neglects to account for many populations. Certain regions may feature more rollover collisions than front facing collisions. The specification from the NBDL sled test helps tailor to frontal collisions. However, this will not benefit many regions of the world. Additional research must be carried out to account for many types of omnidirectional loading conditions that represent collisions in all aspects of the world.

An additional global concern is the difficulty communicating with other countries. There may be relaxed standards in many countries because of the government or societal norms. If a significant research finding is identified, it is ethically important to spread this information as much as possible to manufacturers sending products to more remote areas of the world. Along this same idea, it is very difficult to establish a global standard for ethical responsibilities. Due to different cultures, systems of beliefs, and life experiences, populations will disagree on standards for vehicle safety. Therefore, when establishing a dummy neck in America, it may be considered disrespectful in certain cultures to intervene to maintain the safety of others. This difficulty would make widespread application of a vehicle neck difficult. Furthermore, there is distrust between nations. If the USA created a new dummy neck, other countries might be hesitant to implement the product solely due to the country of origin. This pattern would also apply in a reverse scenario.

Economic

When understanding the ethical and professional responsibilities in engineering design, economic context is important throughout the entire design process. The first major economic consideration is the issue with budgeting and avoiding unreasonable contributions from third parties. Engineers should not offer, give, solicit, or receive any contribution to influence the design process or the design work being completed. Engineers should also avoid accepting commissions from entities dealing with clients or employers of the engineer in connection with the work they are involved in. With regards to budgeting, it is important that engineers are transparent on the spending used on the design process and should not be taking a portion out of the design budget for personal reasons. Another aspect relating to economic considerations is the economy of production and manufacturing is a consideration to be made during the design process. This may involve the costs of producing the neck design, which affects the choices of materials used in the neck dummy. In addition, to reduce manufacturing costs, appropriate design decisions should be made based on the ease of assembly of the neck

dummy. A simpler assembly would make it easier to assemble the final product and streamline the production cycle. This could help with mass production, which would decrease the costs of production. Another economic consideration is costs associated with prototyping and testing designs. In this design project, the use of LS-PrePost and LS-DYNA greatly reduced the cost of the design process. By using finite element analysis and computational methods, the team was able to test different designs without physically building prototypes. While there are also limitations involved with using computational modeling, including divergences from testing the device in real life, these could be mitigated by comparing simulation data to literature values and performance specifications and conducting convergence studies.

Environmental

Engineers have the responsibility of protecting the environment throughout the design process. This includes complying with laws governing environmental matters and managing the amount of carbon or toxic emission during the design and manufacturing processes. During the design process, engineers must ensure the safety, health, and welfare of the public in the context of the environment. This may involve reducing the pollution generated from the manufacturing process and ensuring that waste from the design process will be properly handled and will not pose a threat to the health of humans and the environment. When designing the neck dummy, it is important to consider the materials used during the design process and ensure that the production of the neck dummy will not cause unintended harm to the environment. For example, when 3D printing the prototypes, it is important to ensure only the necessary parts are printed to avoid wastefulness and depletion of shared resources. In addition, it was important to consider how the final product would be manufactured, it is important to note the environmental impact of certain materials being used including its reusability and source. In the final design, the materials being used are butyl rubber, ABR rubber, titanium, and steel, are all reusable materials and non-toxic to the environment. Different aspects of the life cycle of the neck dummy should be accounted for, including easy disassembly for recycling, waste minimization, efficient use of resources, and energy-efficient products.

Societal

One of the biggest issues faced in the initial determination of performance specifications was a lack of available biomechanical data. A large contributing factor to this issue is the small handful of pediatric specimens that have been available for biomechanical testing. From a social perspective, the death of a child is one of the most difficult situations a parent can face. In most cases, these parents are understandably more focused on preserving the memory of their child rather than contributing the body to science for research purposes. In this way, it is an engineer's ethical responsibility to make the most out of the limited number of specimens that are available. The specimen must be handled with care and precision to provide the largest amount of information possible while respecting the memory of the child and wishes of the parents. If parents are able to see that a tragedy can become an avenue to create positive change, this could encourage other families to contribute if they find themselves in a similar situation. This will lead to more data that can ultimately be used to create more detailed performance specifications to prevent other families from experiencing similar tragedies.

Convergence Study

A convergence study was conducted for the final neck under tensile loading to observe if the mesh size of 3.0 mm must be refined. The mesh sizes of 1.5, 2.0, 2.5, 3.0, and 3.5 mm were

subject to tensile loading, and Table 9 details the CPU runtimes and maximum forces experienced during the tests. Additionally, Figure 30 illustrates the relationship between cpu runtime and maximum force. The convergence study details the maximum force begins to converge at a mesh size near 2.0 mm. This mesh size resulted in a simulation time of approximately 8 hours. This is a reasonable runtime that would merit adjusting the mesh size of the final design closer to 2.0 mm in future iterations. Exceeding the mesh size of 2.0 mm began to result in diminishing returns with respect to excessively long runtime approaching 2 days. The slight enhancement of the mesh accuracy is trivial compared to the loss of time to run each iteration. Therefore, a mesh size of 2.0 mm appears to be the optimal mesh for the final neck design.

Table 9. Convergence Study Results

Mesh Size (mm)	CPU Runtimes (s)	Maximum Force (N)
1.5	84250	1018.86
2.0	28626	1109.72
2.5	16094	1282.96
3.0	3610	1364.28
3.5	6192	1505.90

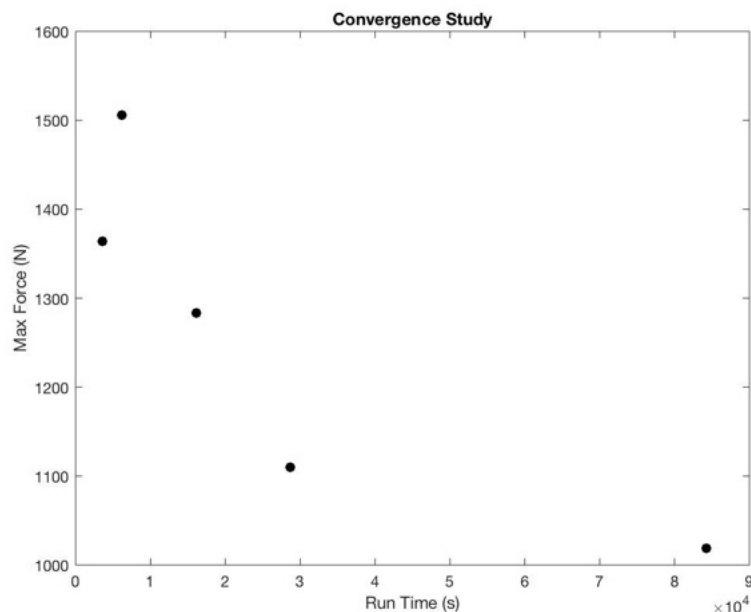


Figure 30. Convergence Study Results

Max Stresses

Likely points of failure for the neck model were determined by analyzing the Von Mises stresses through LS-PrePost's FComp function. The Von Mises stresses were determined for tension and NBDL testing. Under tension, the greatest stress of the neck occurs at the top neck rubber at the greatest neck displacement point. Specifically, it occurs at the top neck rubber point above the prongs, where the rubber displays the lowest cross-sectional area. Figure 31 displays the neck under tension at the point of largest displacement where the middle of the top neck rubber experiences the most stress. This upper rubber segment would be the most likely to fail under tensile loading. The failure would occur at the midpoint between the top of the rubber and where the prongs end.

Under NBDL testing, the max stress in Figure 32 is experienced by the neck before the head collides into the torso. After that point, Von Mises' stresses begin to decrease gradually. Before head collision into the torso, the greatest stress is experienced by the posterior side of the middle rubber around the posterior prongs. The ABR rubber appears to experience the largest load due to the nature of the rigid connection between the titanium prongs and the upper butyl rubber segment. In reality, the most likely failure would be the connection between the prongs and the rubber. However, in the ideal simulation, the ABR rubber would fail on the posterior end.

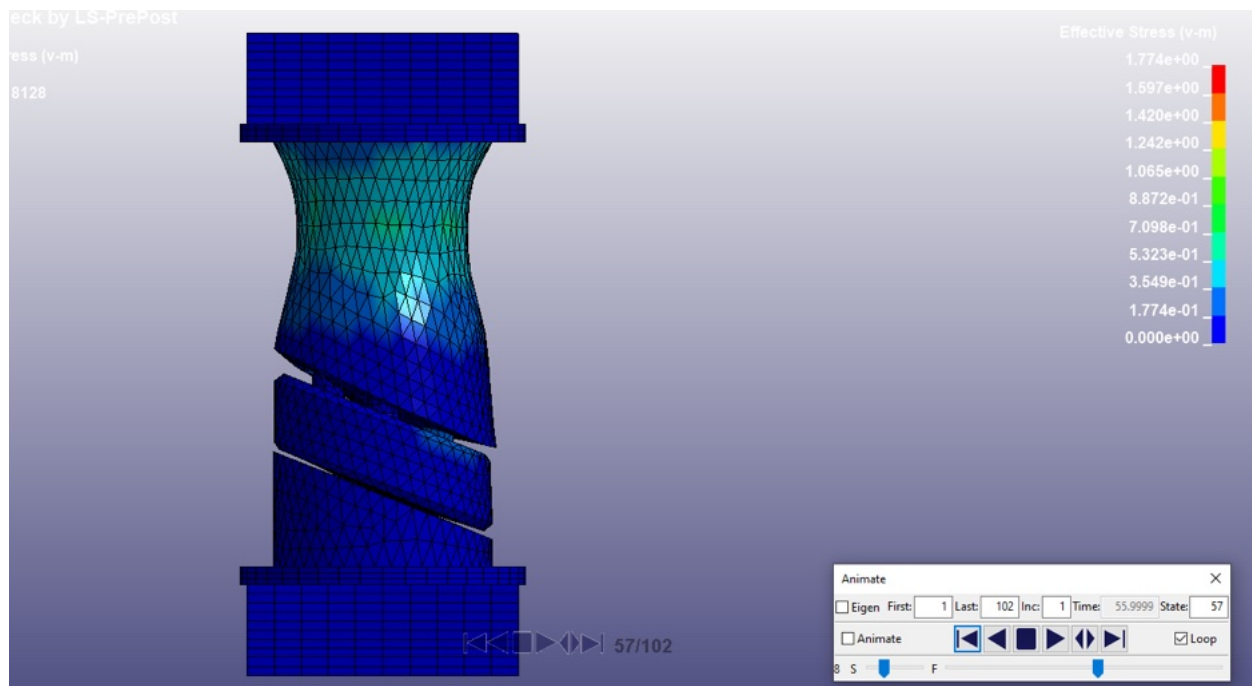


Figure 31. Von Mises' Stress under tension testing

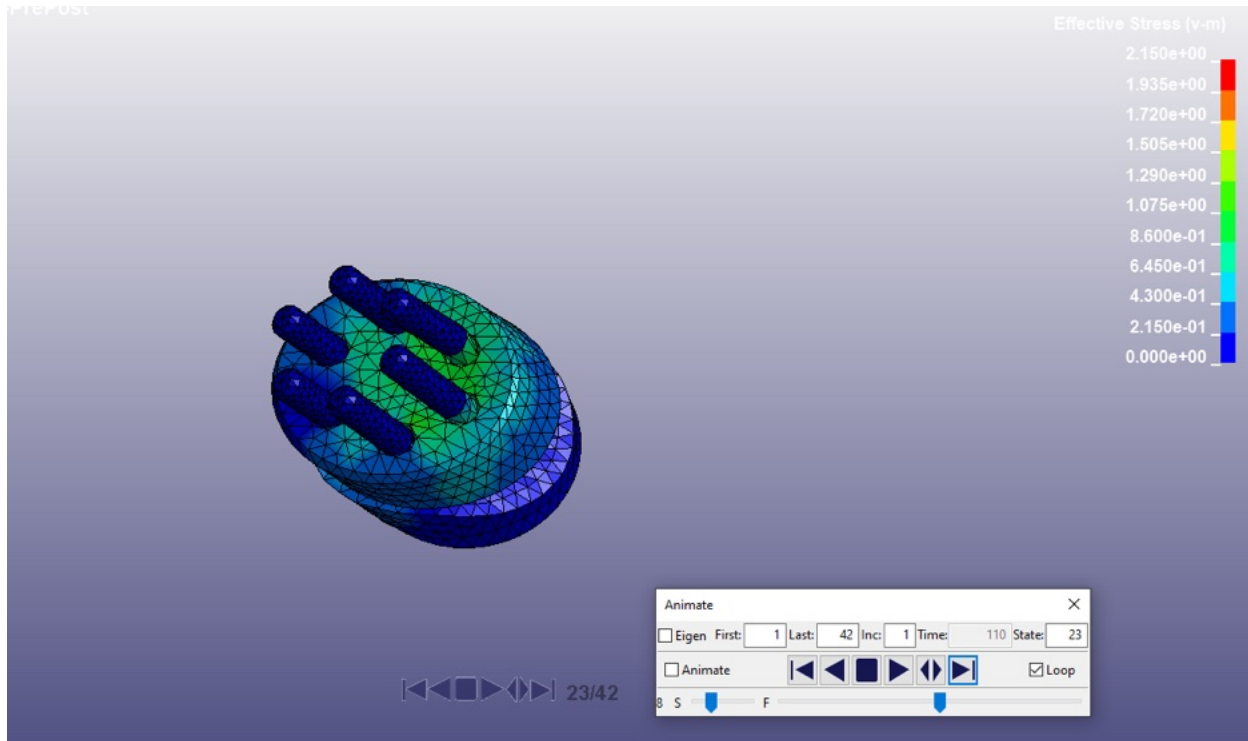


Figure 32. Von Mises' Stress under NBDL testing

Future Modifications to Final Neck Design

The most significant adjustment moving forward would be to add revolute and translational joints. However, if the team were to restart the project, there is a consensus regarding implementing simpler modular designs. Inspired by the teams within class, it would be easier to make adjustments to the design if there were not complex attachments and that could not easily be understood when adjusted. Figure 33 details the complex mindset of the team moving forward.

To enhance the biofidelity of the neck, a revolute joint on the superior end of the neck would adjust the head rotation to be more desirable. Once the NBDL behavior is honed, translational joints on the top and bottom of the neck could be added to match the corridors. The iterations detailed above show promise that with more time, the fine tuning could be performed to maximize the biofidelity of the neck. Additionally, to increase the strain stiffening behavior of the neck under flexion and extension, titanium inserts would be added to the anterior and posterior regions of the neck to stiffen at larger displacements. With an additional semester, a materials comparison could be performed to identify a better viscoelastic material that is less stiff than ABR rubber or butyl rubber at lower impact severities in the CHOP test. This would allow the neck to meet the NBDI and CHOP corridor. The combination of joints, metal inserts, and new materials would be the primary area for modification with additional time to maximize the biofidelity of the neck.

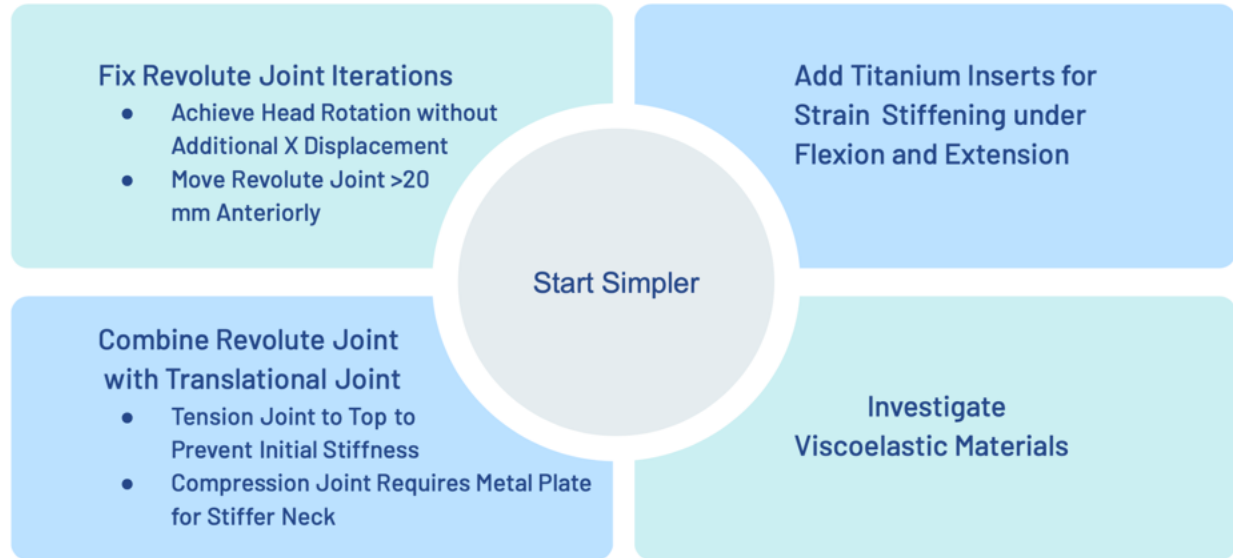


Figure 33. Future Changes to Final Neck Design

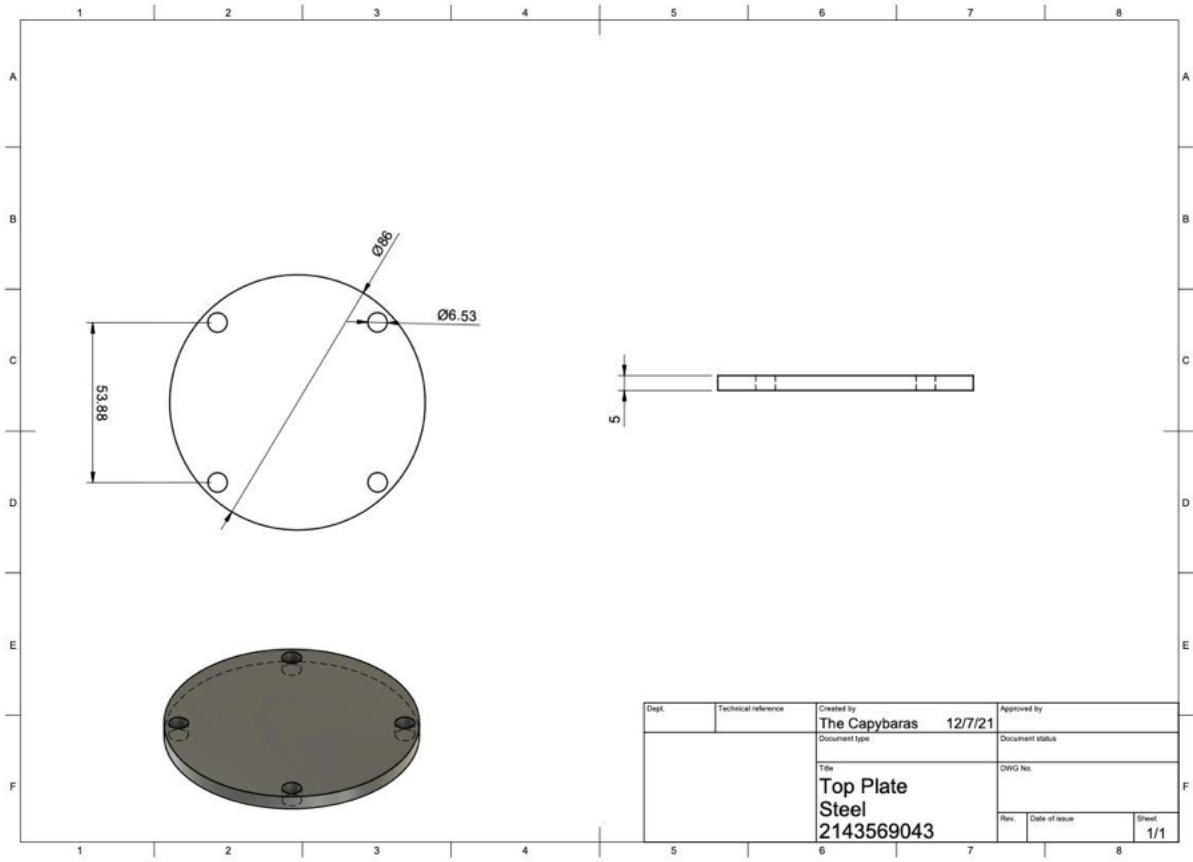
Appendix

Appendix A: Project Description

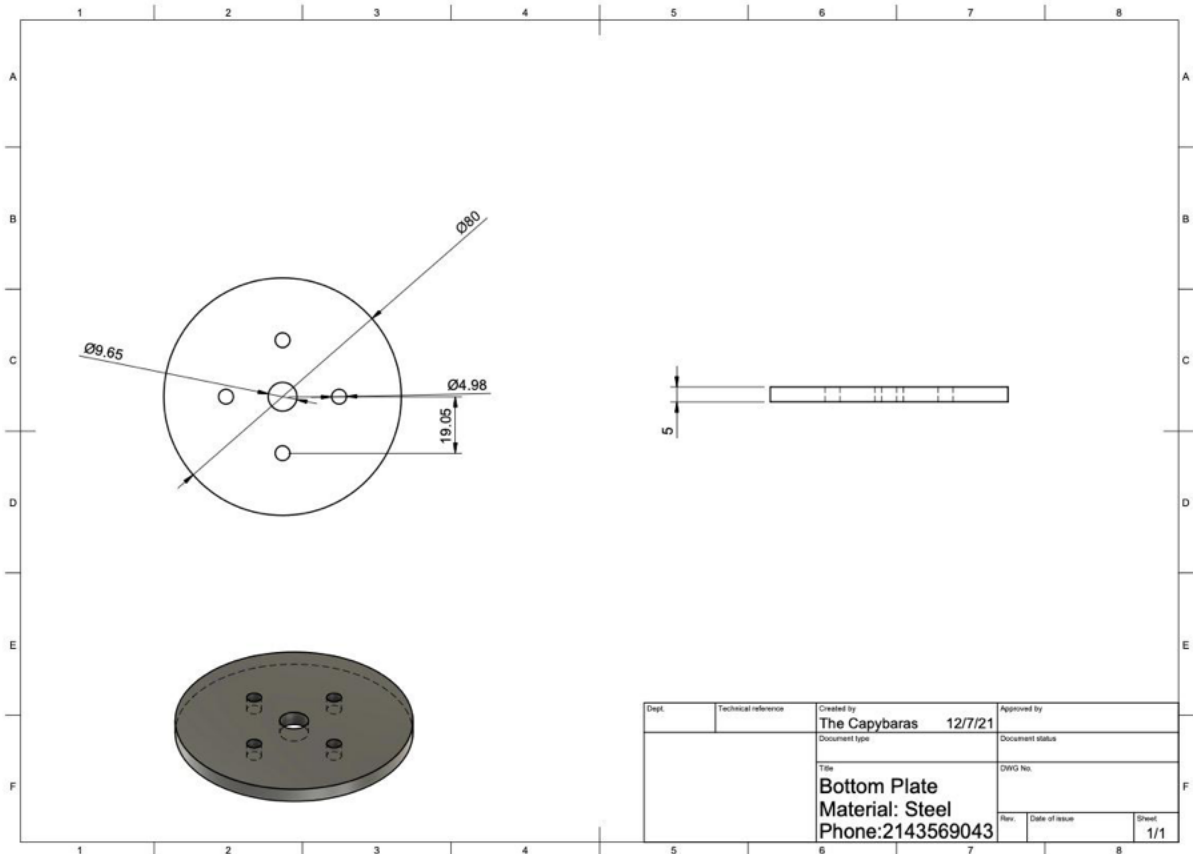
Over the course of several decades, the automobile industry has made occupant safety a top priority in vehicle design. This has been accomplished by creating vehicle safety standards that are verified in large part through the use of anthropomorphic test devices (ATDs). However, for these standards to be able to protect the population as intended, the ATDs used in testing must consistently and accurately represent the biomechanical behaviors that would be expected out of their human counterparts. This is an issue faced by the current 6-year-old ATD neck, the Hybrid III, which is considered to be generally too stiff and not fully representative of the physical characteristics of the pediatric neck. Here, we present a slanted neck design made up of butyl rubber, ABR rubber, and titanium prongs. This design was iterated and verified through the use of tension, compression, bending, and sled testing simulations in LS-DYNA.

Appendix B: Final Neck Design Engineering Drawings

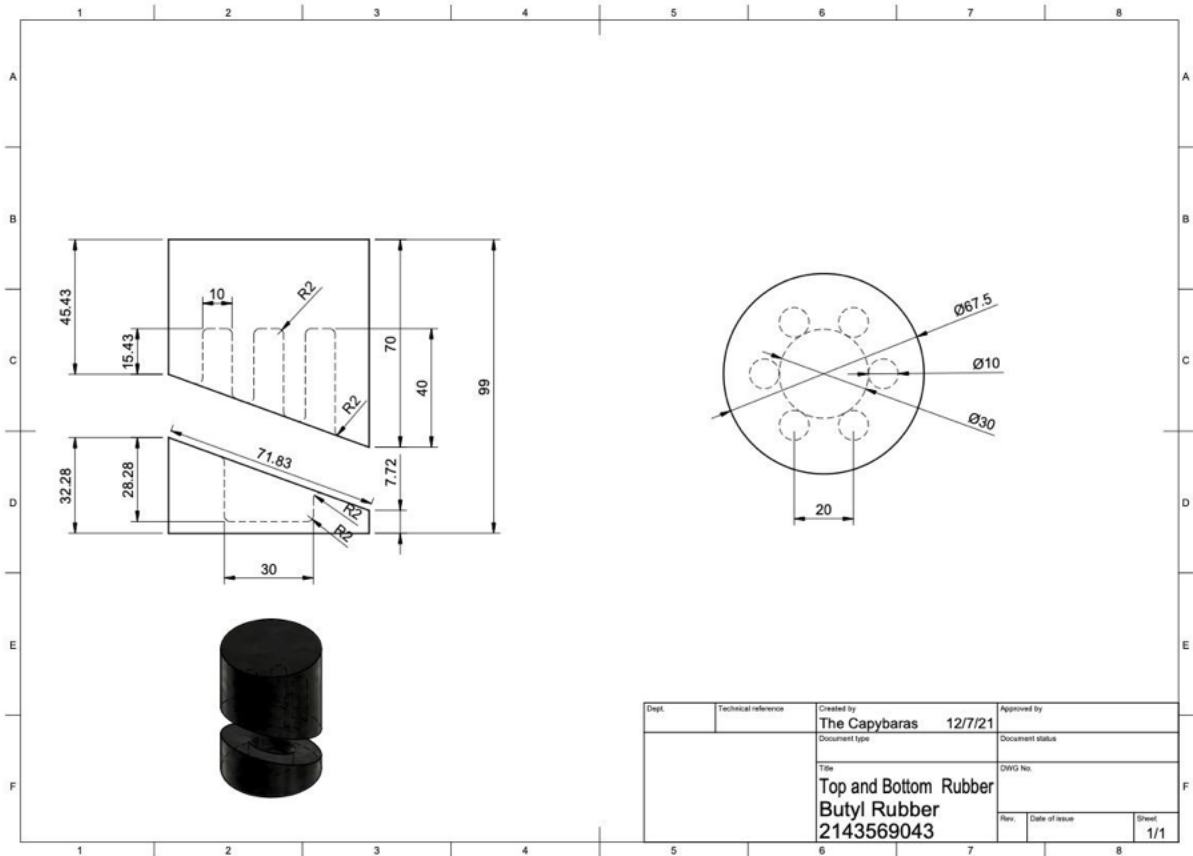
Top Plate



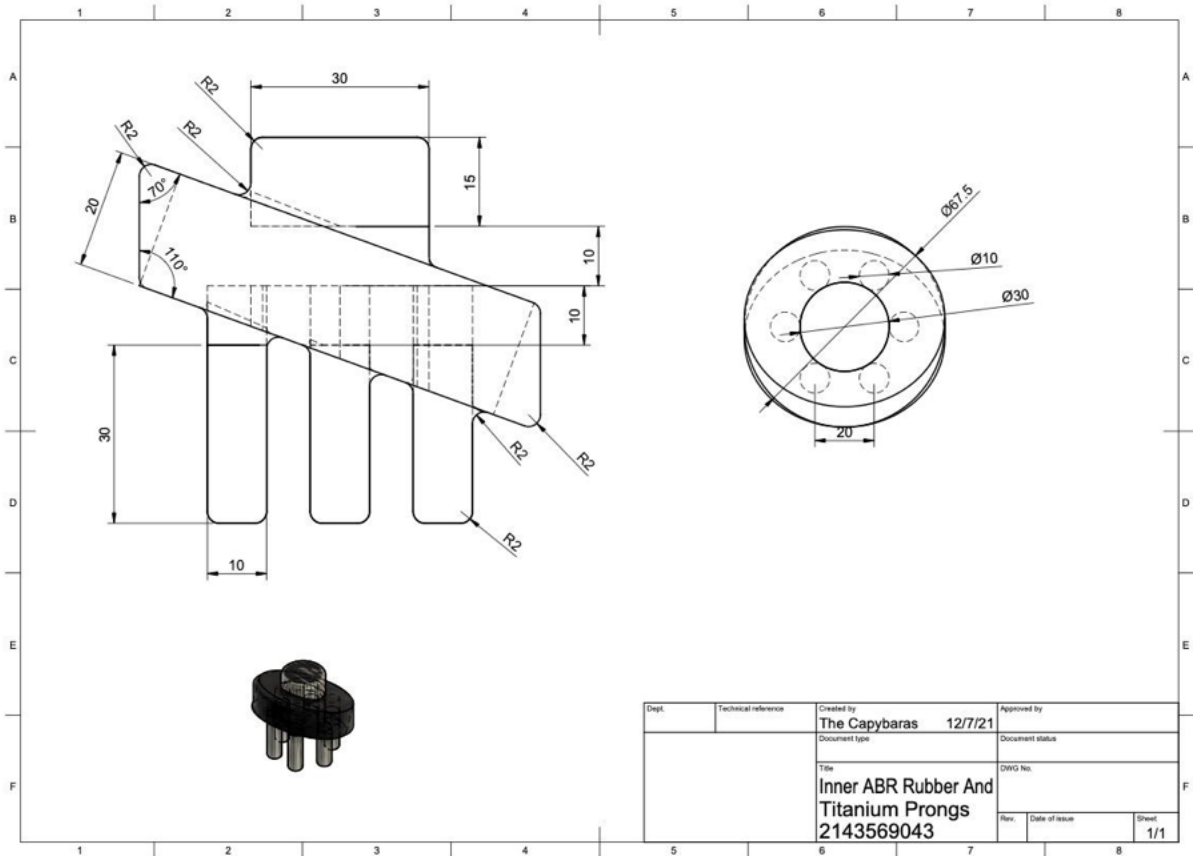
Bottom Plate



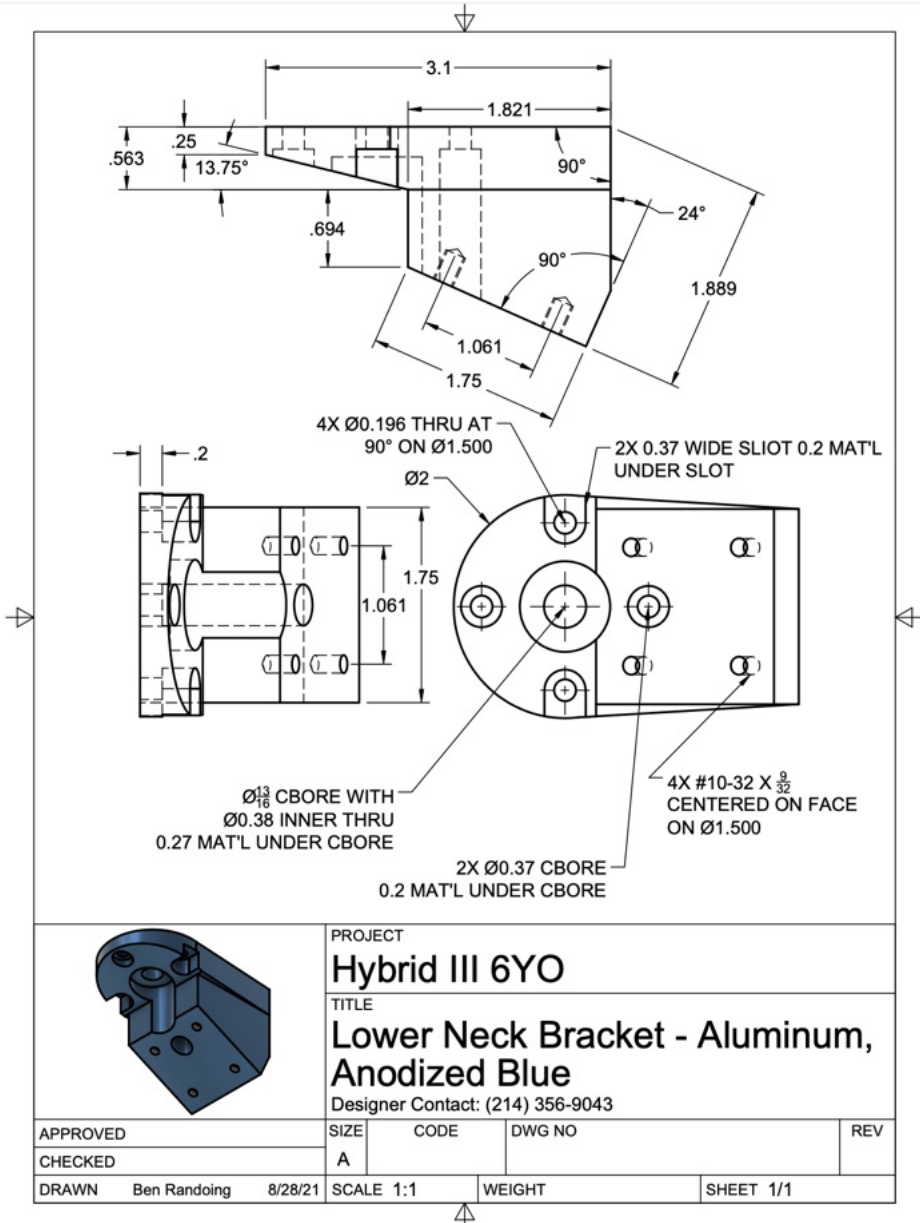
Top and Bottom Rubber



Inner ABR Rubber Disc with Titanium Prongs

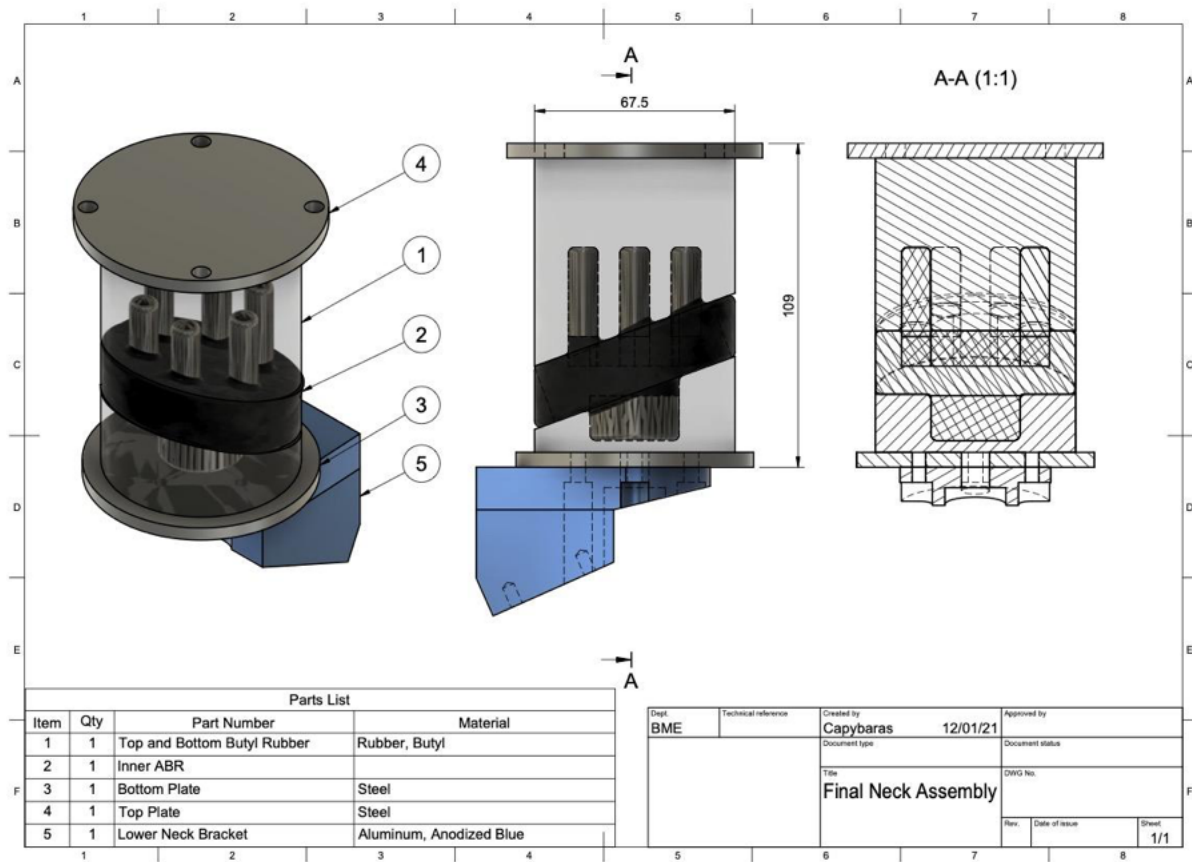


Lower Neck Bracket

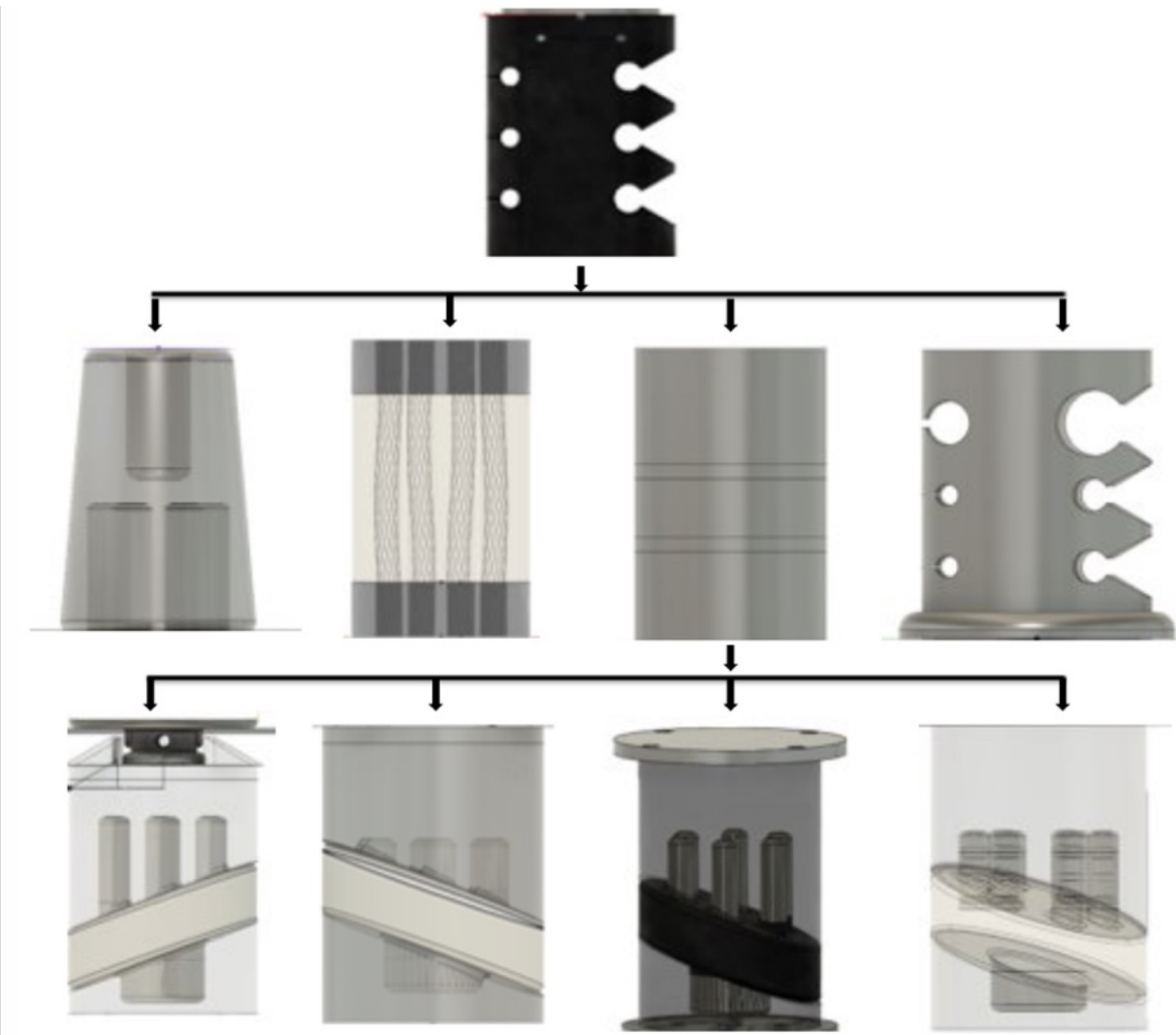


Assembly Drawing

The material of the Inner Disc is ABR Rubber and the prongs are Titanium.

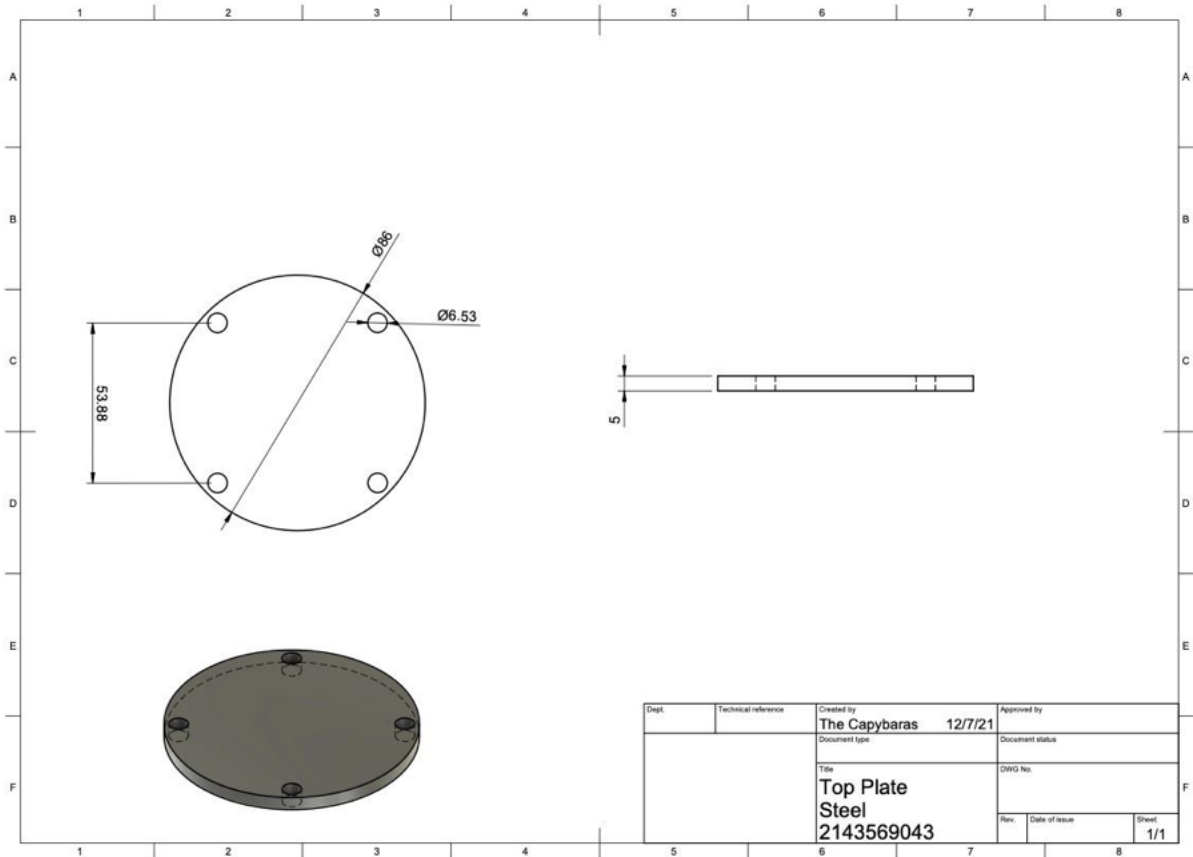


Appendix C: Design Iteration Work Flow Schematic

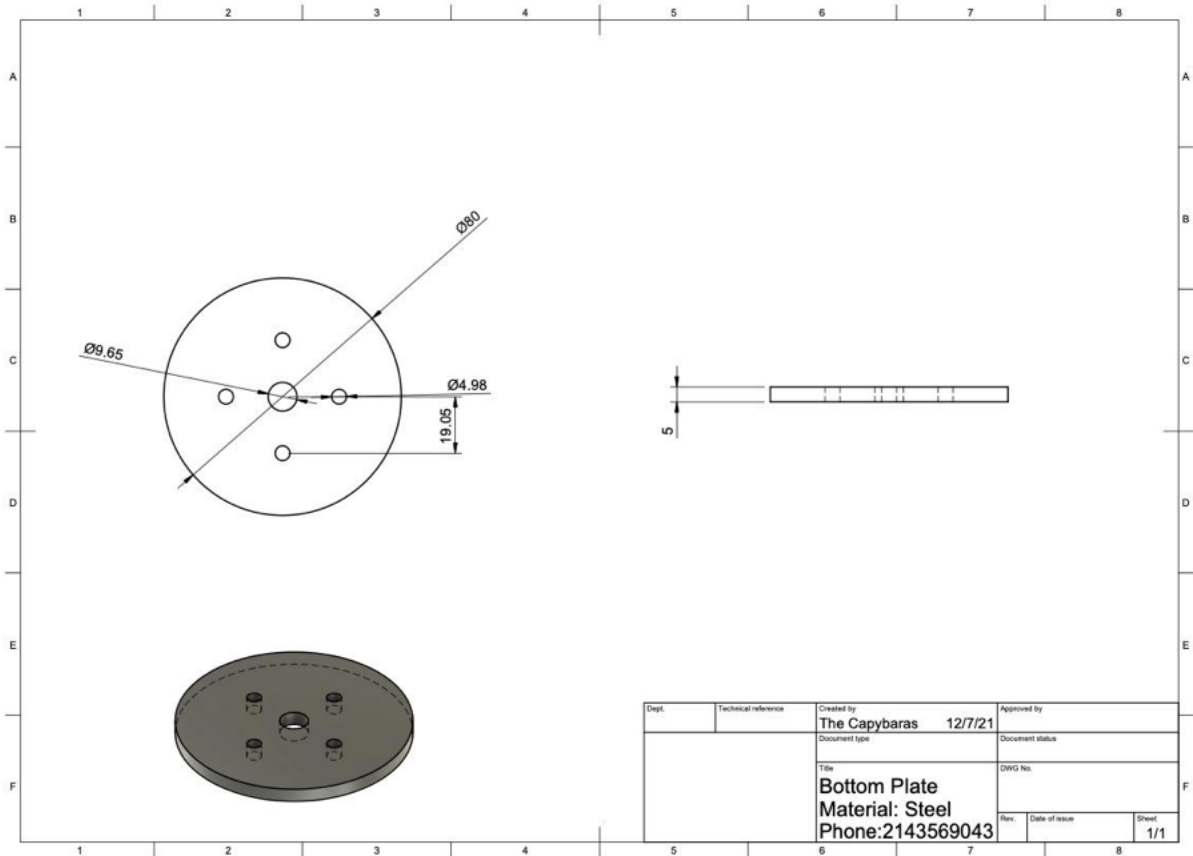


Appendix D: Revolute Joint Iteration Engineering Drawings

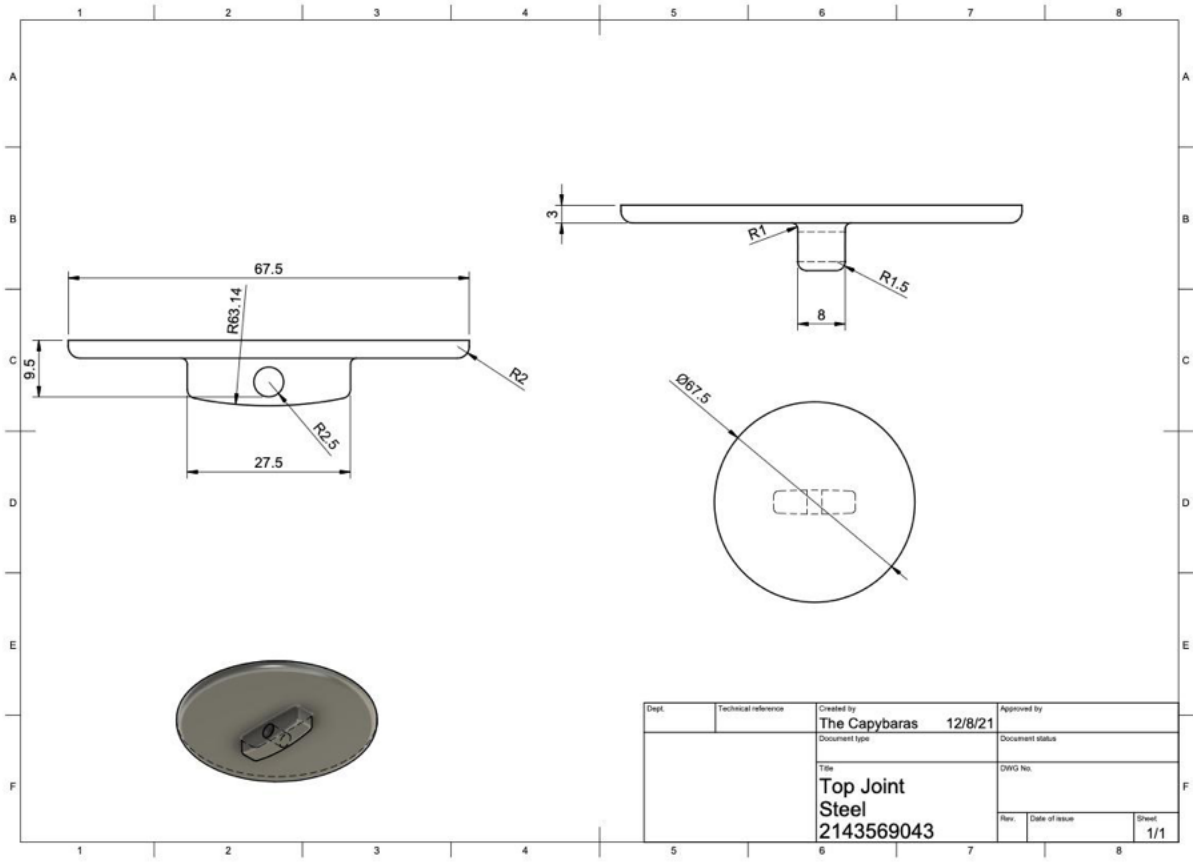
Top Plate



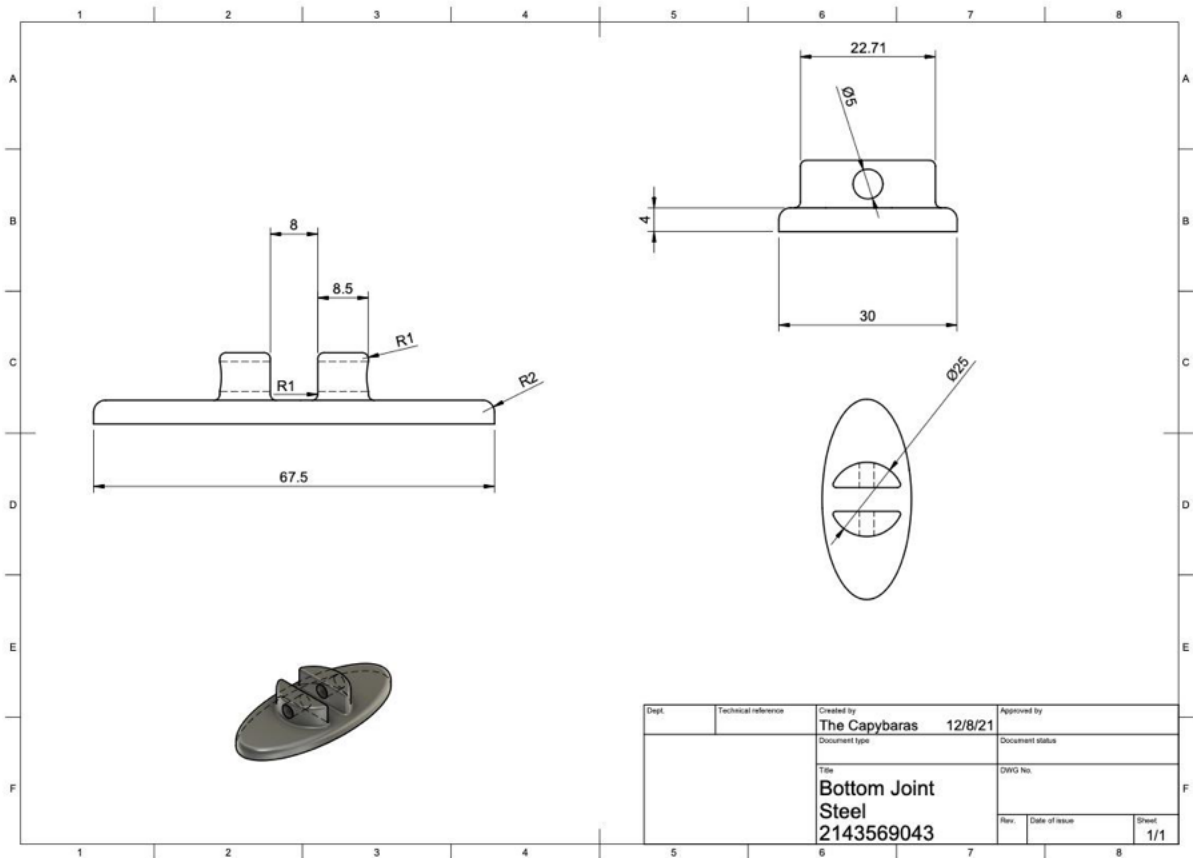
Bottom Plate



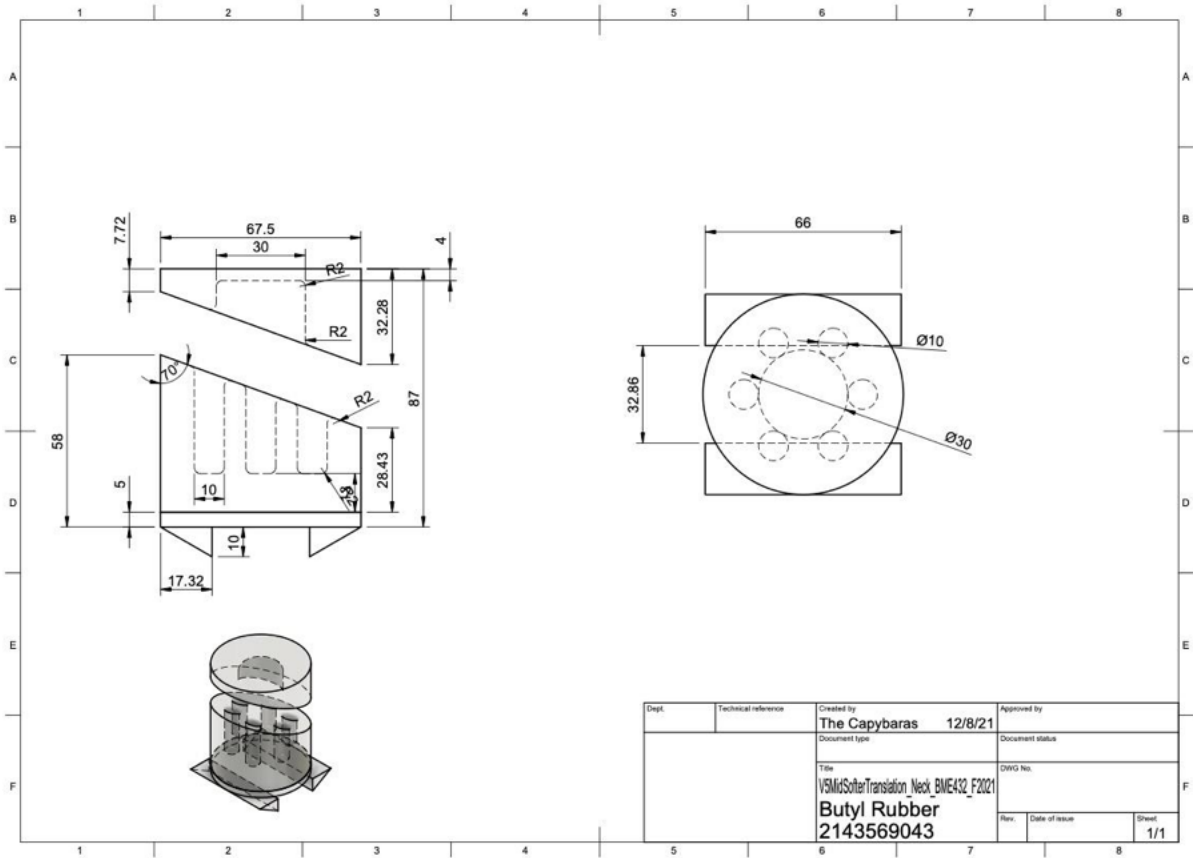
Top Joint



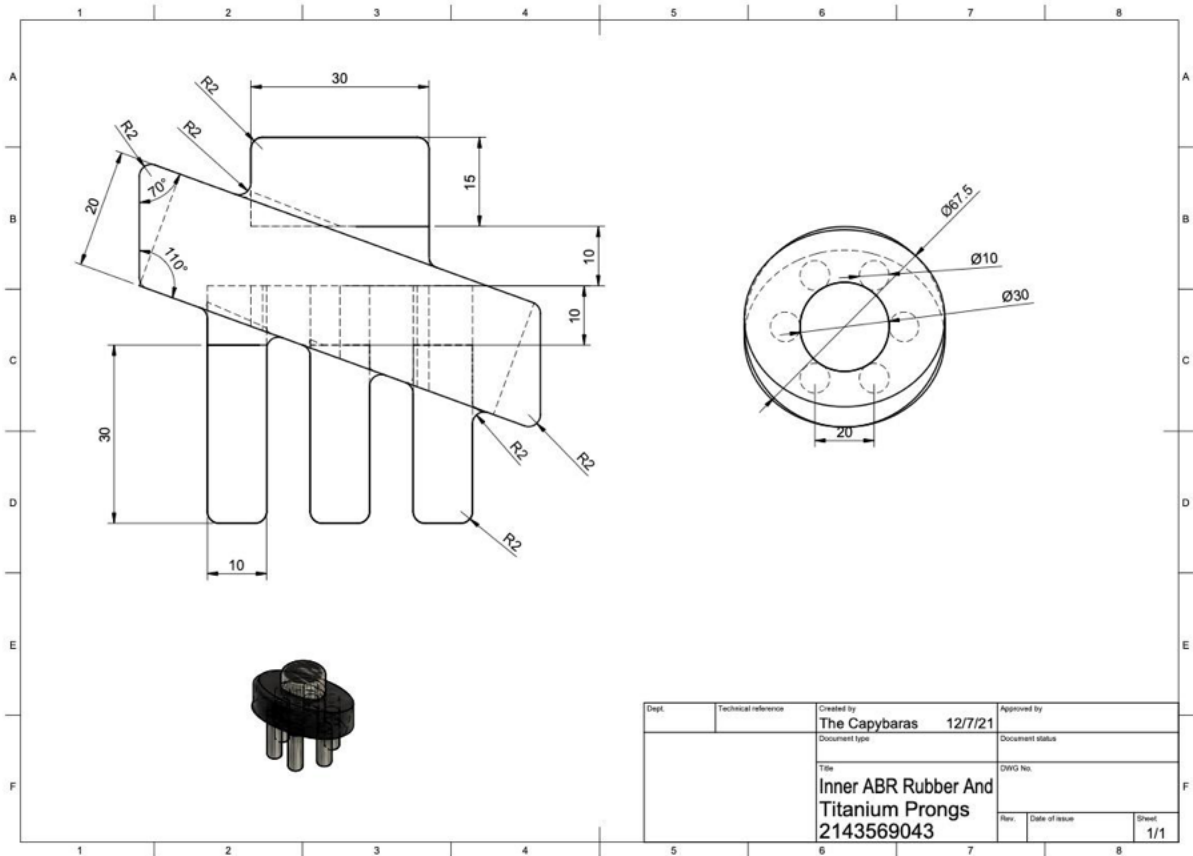
Bottom Joint



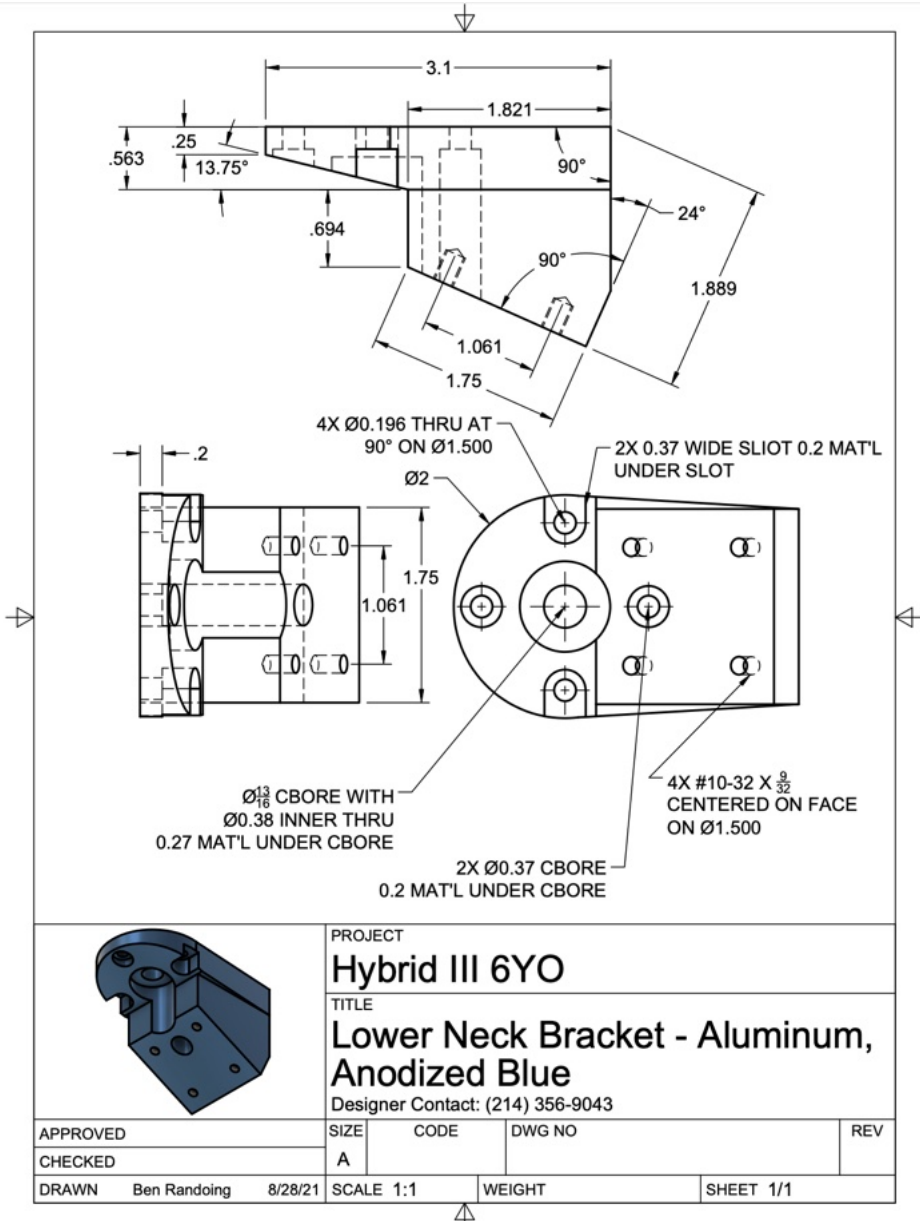
Upper and Lower Butyl Rubber



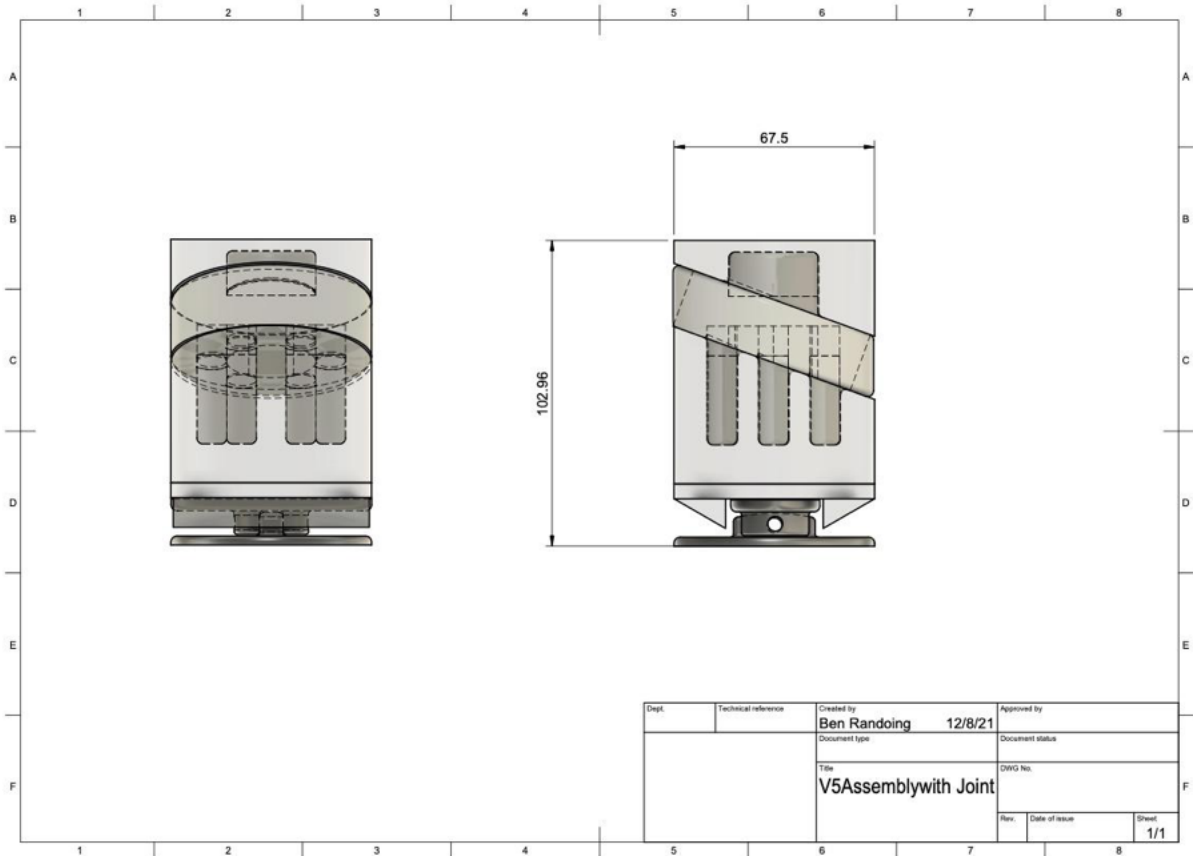
Mid ABR and Titanium Prongs



Lower Neck Bracket



Assembly



Appendix E: Corridor Fit Summary

Test	Fit Type	R ² UC	R ² LC	R ² mean
Tension	3rd Degree Fourier	1	1	1
Compression	7th Degree Fourier	1	1	1
CHOP EAMX	7th Degree Fourier	0.9999	0.9994	0.9997
CHOP EAMZ	5th Degree Fourier	0.9997	0.9998	0.9999
CHOP NASX	7th Degree Fourier	0.9999	0.9996	0.9998
CHOP NASZ	7th Degree Fourier	1	1	1
CHOP Rotational Velocity Y	5th Degree Fourier	0.9951	0.9926	NA
NBDL Head Lag	7th Degree Fourier	0.9999	0.9999	0.9999
NBDL CG Displacement	3rd Degree Fourier	0.9997	0.9992	NA
NBDL CGx Timing	NA	NA	NA	NA
NBDL CGz Timing	NA	NA	NA	NA
Extension	1 Term Exponential	1	1	1
Flexion	Linear Piecewise	NA	NA	NA